Coexistence policies in cognitive radio

Mario Lopez Martinez   Supervisor: Juan Jose Alcaraz Espin

01 March 2015*

*First drafted on 28 November 2014

Contents

List of Figures

List of Tables

Introduction

Part I

Dynamic Spectrum Access

CHAPTER 1

Background Detection of Primary User Activity in Opportunistic Spectrum Access

1.1 Introduction

Motivation

One of the main problems of opportunistic spectrum access, OSA, is that current radio frequency front-ends cannot perform sensing and transmission in the same channels at the same time. In consequence, in OSA protocols, spectrum sensing and SU data transmission are performed in two separated phases. The scanning phase allows the SUs to find spectrum holes to transmit in. However, during the transmission phase, a channel occupied by an SU can be eventually used by a PU transmission (transmission overlap) causing a potentially harmful interference to the PU receiver. To solve this problem, the SU is only allowed to transmit during a limited amount of time after which it leaves the channel or performs a new sensing procedure (periodic sensing).

OSA with periodic sensing ([165], [166], [167], [168], [169], [170]) consists of a sensing period followed by a transmission period. These two separated periods are sometimes referred to as the medium access control (MAC) frame. In general, a longer sensing duration improves the sensing quality, but the higher sensing overhead in the MAC frame reduces SU throughput. The duration of the transmission period has also influence on the SU throughput and the probability of collision with PU transmissions. The throughput-collision tradeoff is present in [165] and [166], where joint designs of the sensing and access strategy are proposed. For a fixed frame duration, [167] optimizes the sensing time to improve the SU throughput under detection quality constraints. In contrast, [168] considers a fixed sensing time and optimizes the transmission duration subject to an interference power constraint. Both sensing and transmission times were jointly optimized in [169] and

[170]. One of the main contributions of the latter is to consider the impact of imperfect sensing on the throughput of secondary users as well.

The OSA model of these works constitute the base upon which we develop our proposal. We assume a system in which the sensing period is long enough to find, with a sufficiently high reliability, an available channel to transmit in. According to a given PU activity model, the length of the SU transmission period is set to the value that maximizes the SU throughput under the desired collision probability constraint. This is a worst case PU QoS criteria used in multiple previous works ([166], [170], [148], [149], [144]), which considers that any collision causes harmful interference to PU receivers. As in [170], our model also includes the effect of transmission overlap in SU performance. Additionally, we use the statistical description of the fading in the direct and interference links to evaluate this performance. The generic OSA model described is referred as *optimized OSA* in this paper, and is used as a starting point and as a benchmark for our proposal. As in [166], [148], [144], [145], [150], the transmission period is divided into time slots. Each time slot contains one SU data packet transmission.

In [171] it is assumed that, whenever an SU and a PU transmit simultaneously, both experience collision and the SU can detect the collision after the transmission. Perfect collision detection is also implicitly assumed in [172].

In this paper, we relax the perfect collision detection assumption, taking into consideration the multiple factors that hinder perfect detection: pathloss, fading effects, and decoding probability as a function of the modulation used and the signal-to-interference-and-noise ratio. To overcome these difficulties and perform an optimal collision detection, the SU receiver can make use of diverse estimations performed during the successive spectrum scanning and sensing periods: average PU received power, statistical characterization of the fading process, and PU traffic pattern. As an example, an accurate PU traffic estimator is described in [173].

Our Contribution

We propose a collision detection mechanism that performs PU activity estimation during SU packet reception, and use it to improve the classic optimized OSA mechanism. We refer to this mechanism as *background detection* (BD). In contrast to classic spectrum sensing, where licensed channels are sensed while the SU transmitter is idle ([164]), the BD mechanism operates only at the SU receiver, during ongoing SU transmissions. In consequence, BD uses the information available at the SU receiver during packet reception: power levels, and the presence or absence of decoding errors, to decide, by means of a maximum a posteriori (MAP) estimator, if there has been overlap in each transmission slot. The MAP estimator exploits existing knowledge at the SU, such as the average received powers, the PU traffic pattern and the statistical description of the fading processes. We also evaluate the robustness of the system under inaccuracies in these data. In particular, it is shown that, while optimized OSA is very reliant on an accurate PU traffic characterization, optimized OSA with BD presents higher robustness against PU traffic misestimations.

The rest of this paper is organized as follows. Section 1.2 describes the PU and SU networks and presents the technical foundations of the proposal. Section 1.3 discloses the background detection mechanism, formulating the MAP rule and then computing the detection probabilities. Section 1.4 develops Markov models for the optimized OSA with and without BD. Combining these models with simulations, we present, in Section 1.4 a numerical evaluation of BD performance and robustness.

1.2 System Description

General Considerations

The mechanism proposed in this paper is very generic, and is applicable whenever the primary and the secondary wireless networks present some general characteristics described in this section. The spectrum of the primary network is assumed to be divided into orthogonal channels, so that primary transmissions are multiplexed on these channels (e.g. TDM, FDM, OFDMA). The SU can therefore scan these channels, monitor PU activity and detect spectrum opportunities in them. The SUs are also capable of estimating the PU traffic pattern on these channels. One type of PU access networks that fit well on this description are cellular networks, but other types may be feasible for our proposal as well.

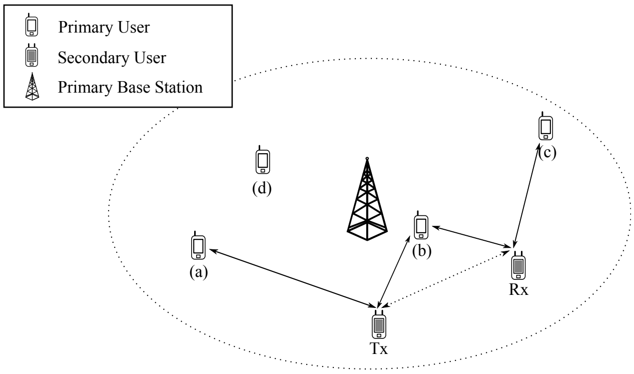

Figure 1.1: Example of the system under study.

As an example, let us consider the system in Figure 1.1, representing the coverage area (cell) of a PU base station (PU BS), where a cognitive pair (CP), consisting of an SU transmitter (SU Tx) and an SU receiver (SU Rx), tries to perform an SU transmission on a spectrum opportunity within this PU cell. Figure 1.1 also depicts the interference links between the SUs and the PU terminals. Because the SUs are within the range of the PU BS, there is also one interference link from the PU BS to each SU. Before transmitting, both the SU Tx and the SU Rx scan the licensed spectrum looking for available channels and exchange control messages containing their sensing outcomes over a dedicated control channel. Once the CP makes the access decision, the SU Tx starts the SU transmission over one or more available channels. It is assumed that the SU transmits in PU downlink channels. Although the BD scheme could be used for PU uplink channels, it is more effective for downlink channels for the reasons explained in Section 1.5. The SU transmission is divided into time-slots. At the end of each time-slot, the SU Rx submits a control message to the SU Tx over the control channel. In general, this message would contain an ACK (or NACK) of the data transmitted on the time-slot, but our proposal will also include information about the power received at the SU Rx during the time-slot.

It is assumed that the signal power received at the SU Rx remains constant during a symbol time T_s of the SU Tx transmission. In this case, the probability of correct signal detection at the SU Rx is defined in terms of the probability that the signal to interference ratio (SINR) is above a given threshold, which is determined by the minimum acceptable bit error rate (BER) for correct decoding, the transmission rate and the modulation used. Let us consider that, given the SU data packet length, and the information and redundancy bits in it, SU packets are correctly received if the BER during the packet reception is above certain value (e.g. 10^{-3}). This BER objective is attained when the ratio E_b/N_0 is above a threshold γ_b, where E_b is the energy per bit and N_0 is the noise spectral density (including both thermal and interference noise). The threshold depends on the modulation used (e.g. for BPSK, BER $= 10^{-3}$ for $\gamma_b = 7$ dB). Therefore, the threshold in terms of SINR is given by $\gamma = \gamma_b/(BT_b)$ where B is the channel bandwidth and T_b the bit duration.

Principles of the Background Detection Scheme

Each SU data packet may be received at the SU Rx with or without PU interference. Let P denote the signal power at the SU Rx during the reception of an SU data packet. The SU signal is received with power Y at the SU Rx and, in case of transmission overlap, the signal transmitted by the PU BS is received with power X at the SU Rx. Note that P, X, and Y are random variables. Under PU-SU transmission overlap, $P = X + Y$ and, in absence of overlap, $P = Y$. Similarly, the SINR is $\mathtt{SINR} = \frac{Y}{N+X}$, with overlap, and $\mathtt{SINR} = \frac{Y}{N}$ without opverlap, where N denotes the total thermal noise power in the channel bandwidth. If $\mathtt{SINR} > \gamma$ the packet is correctly received and, if $\mathtt{SINR} \leq \gamma$ the packet is impossible to decode (error event).

After the reception of an SU data packet, the SU Rx can obtain two observations: P, and the occurrence (or absence) of an error event. The idea of the background detection (BD) mechanism is to use these observations to allow the SUs estimate the presence of PU activity during SU transmissions. If PU activity is detected, the OSA algorithm may decide to end the ongoing SU transmission to protect from interference any PU terminal in range of the SU Tx (In Figure 1.1, PU terminals a and b) in case any of them is receiving PU BS transmissions on the channel where the overlap was detected.

The BD scheme is essentially a binary hypothesis testing mechanism conducted during SU transmission to decide on the most feasible value of a random variable Θ, which takes two possible values $\{0, 1\}$ at each SU packet reception. The event $\Theta = 1$ indicates that there has been PU interference during the packet reception, and $\Theta = 0$ indicates that the reception was free of PU interference. The probability density functions (PDF) of Y and X are $f_Y(y)$ and $f_X(x)$ respectively. In case that both the SU Tx and the PU BS signals experience Rayleigh fading over their respective links to the SU Rx, we have

$$lclf_Y(y) = \frac{1}{p_{ss}} e^{-\frac{y}{p_{ss}}} \tag{1.1}$$

$$f_X(x) = \frac{1}{p_{ps}} e^{-\frac{x}{p_{ps}}} \tag{1.2}$$

where p_{ss} is the average power received from the SU Tx and p_{ps} is the average power received from the PU BS. Both distributions, as well as the average powers can be obtained from the previous sensing history of the SUs. Similarly, this sensing history provides information about the PU traffic profile and intensity on the scanned channels. One basic metric is the probability of PU activity during the transmission time of an SU packet ($\boldsymbol{P}(\Theta = \theta)$), with $\theta = \{0, 1\}$. Therefore, assuming $f_Y(y)$, $f_X(x)$ and $\boldsymbol{P}(\Theta = \theta)$ are known, the hypothesis testing is based on Bayesian estimation, resulting in a maximum a posteriori probability (MAP) decision rule. In Section 1.5 we evaluate the sensitivity of the BD mechanism to the inaccuracies in the estimation of the PDFs and traffic parameters.

Summarizing, once the SU transmission has started, the SU Rx obtains, upon each packet reception, the following observation:

$$(P, E) = \begin{cases} (p_r, 0) & \text{, if } \mathtt{SINR} > \gamma \\ (p_r, 1) & \text{, if } \mathtt{SINR} \leq \gamma \end{cases} \tag{1.3}$$

And, upon this observation, the MAP decision rule selects the hypothesis having the maximum posterior distribution over the two possible values of θ. Next section provides a detailed derivation for the BD MAP rule, and obtains the probabilities of correct and incorrect detection of the MAP estimator.

1.3 PU Activity Detection in Background

MAP Rule

Given the observation pair, $(P = p_r, E = e)$, the MAP rule selects the hypothesis H_i for which the posterior probability $\boldsymbol{P}(\Theta = \theta | P = p_r, E = e)$ is largest. By Bayes' rule this is equivalent to select the hypothesis maximizing $p_\Theta(\theta) f_{P,E|\Theta}(p_r, e|\theta)$. Because E is a discrete random variable, we have to consider separately each possible value of the outcome e ($e = 0$, if the SU packet is received without errors and $e = 1$ otherwise) for the computation of the posterior probability. Let E_0 and E_1 refer to the events $e = 0$ and $e = 1$ respectively. Similarly, we use H_0 and H_1 to refer to the events $\Theta = 0$ and $\Theta = 1$. Let us derive the expression of $f_{P,E|\Theta}(p_r, e|\theta)$ for each possible combination of E_0 and E_1 with H_0 and H_1.

Case E_1, H_1

Applying the definitions we have

$$\begin{aligned} f_{P,E_1|H_1}(p_r, E_1|H_1) &= \frac{\partial}{\partial p_r}\boldsymbol{P}(P \le p_r, \mathtt{SINR} \le \gamma|H_1) \\ &= \frac{\partial}{\partial p_r}\boldsymbol{P}(X+Y \le p_r, Y \le N\gamma + X\gamma) \end{aligned} \tag{1.4}$$

We will first find the joint PDF of P and X and then integrate to find the PDF of P.

$$\begin{aligned} \boldsymbol{P}(X+Y \le p_r, Y \le N\gamma + X\gamma|X=x) &= \boldsymbol{P}(Y \le p_r - x, Y \le N\gamma + x\gamma|X=x) \\ &= \boldsymbol{P}(Y \le \min(p_r - x, N\gamma + x\gamma)|X=x) \\ &= \boldsymbol{P}(Y \le \min(p_r - x, N\gamma + x\gamma)) \\ &= \int_{-\infty}^{\min(p_r-x, N\gamma+x\gamma)} f_Y(y)dy \\ &= \begin{cases} \int_{-\infty}^{p_r-x} f_Y(y)dy & \text{, if } p_r \le N\gamma + x(\gamma+1) \\ \int_{-\infty}^{N\gamma+x\gamma} f_Y(y)dy & \text{, otherwise} \end{cases} \end{aligned} \tag{1.5}$$

where the third equality comes from the independence of the PU and SU signals, X and Y. By differentiating both sides with respect to p_r we obtain

$$f_{P,E_1|H_1,X}(p_r, E_1|H_1, x) = \begin{cases} f_Y(p_r - x) & \text{, if } p_r \le N\gamma + x(\gamma+1) \\ 0 & \text{, otherwise} \end{cases} \tag{1.6}$$

Then, the joint PDF of P and X is

$$\begin{aligned} f_{P,X,E_1|\Theta}(p_r, x, E_1|H_1) &= f_{X|\Theta}(x|H_1)\, f_{P,E_1|\Theta}(p_r, E_1|H_1) \\ &= f_X(x)\, f_{P,E_1|\Theta}(p_r, E_1|H_1) \\ &= \begin{cases} f_X(x)\, f_Y(p_r - x) & \text{, if } p_r \le N\gamma + x(\gamma+1) \\ 0 & \text{, otherwise} \end{cases} \end{aligned} \tag{1.7}$$

from which we finally obtain

$$\begin{aligned} f_{P,E_1|H_1}(p_r) &= \int_{-\infty}^{\infty} f_{P,X,E_1|\Theta}(p_r, x, E_1|H_1)\, dx \\ &= \int_{\frac{p_r - N\gamma}{(1+\gamma)}}^{\infty} f_X(x)\, f_Y(p_r - x)\, dx \end{aligned} \tag{1.8}$$

where $f_{P,E_1|H_1}(p_r)$ denotes $f_{P,E_1|H_1}(p_r, E_1|H_1)$ in a more compact form. When both links are characterized by Rayleigh fading, $f_X(x)$ and $f_Y(y)$ are exponential distributions and we have

$$f_{P,E_1|H_1}(p_r) = \begin{cases} \dfrac{e^{-\frac{p_r}{p_{ps}}} - e^{\left(-\frac{p_r}{p_{ss}} + \frac{(p_{ps}-p_{ss})(p_r - N\gamma)}{p_{ps}p_{ss}(1+\gamma)}\right)}}{p_{ps} - p_{ss}} & \text{, if } p_r \ge N\gamma \\ \dfrac{e^{-\frac{p_r}{p_{ps}}} - e^{-\frac{p_r}{p_{ss}}}}{p_{ps} - p_{ss}} & \text{, otherwise} \end{cases} \tag{1.9}$$

Case E_0, H_1

Proceeding similarly to the case above we have

$$\begin{aligned} f_{P,E_0|H_1}(p_r, E_0|H_1) &= \frac{\partial}{\partial p_r} \boldsymbol{P}(P \le p_r, \mathtt{SINR} > \gamma | H_1) \\ &= \frac{\partial}{\partial p_r} \boldsymbol{P}(X + Y \le p_r, Y > N\gamma + X\gamma) \end{aligned} \tag{1.10}$$

To obtain the joint PDF of X and P we need the following probability

$$\begin{aligned} \boldsymbol{P}(X + Y \le p_r, Y > N\gamma + X\gamma | X = x) &= \boldsymbol{P}(X + Y \le p_r, Y > N\gamma + X\gamma) \\ &= \boldsymbol{P}(N\gamma + X\gamma < Y \le p_r - x) \\ &= \begin{cases} \int_{N\gamma+X\gamma}^{p_r - x} f_Y(y)dy & \text{, if } x < \frac{p_r - N\gamma}{1+\gamma} \\ 0 & \text{, otherwise} \end{cases} \end{aligned} \tag{1.11}$$

By differentiating with respect to p_r we obtain

$$f_{P,E_0|H_1,X}(p_r, E_0|H_1, x) = \begin{cases} \frac{\partial}{\partial p_r} \int_{N\gamma+X\gamma}^{p_r - x} f_Y(y)dy & \text{, if } x < \frac{p_r - N\gamma}{1+\gamma} \\ 0 & \text{, otherwise} \end{cases} \tag{1.12}$$

Then, after obtaining the joint PDF of X and P, we integrate over x to get

$$f_{P,E_0|H_1}(p_r) = \int_{-\infty}^{\frac{p_r - N\gamma}{1+\gamma}} \left(\frac{\partial}{\partial p_r} \int_{N\gamma+X\gamma}^{p_r - x} f_Y(y)dy \right) f_X(x)dx \tag{1.13}$$

which, for Rayleigh fading has the following form

$$f_{P,E_0|H_1}(p_r) = \begin{cases} \frac{1}{p_{ps} - p_{ss}} e^{-\frac{p_r}{p_{ss}}} \left(e^{\frac{(p_{ps} - p_{ss})(p_r - N\gamma)}{p_{ps} p_{ss}(1+\gamma)}} - 1 \right) & \text{, if } p_r > N\gamma \\ 0 & \text{, otherwise} \end{cases} \tag{1.14}$$

Case E_1, H_0

In this case there is no signal received from the PU and the conditional PDF of P is defined as follows

$$\begin{aligned} f_{P,E_1|H_0}(p_r, E_1|H_1) &= \frac{\partial}{\partial p_r} \boldsymbol{P}(P \le p_r, \mathtt{SINR} \le \gamma | H_1) \\ &= \frac{\partial}{\partial p_r} \boldsymbol{P}(Y \le p_r, Y \le N\gamma) \end{aligned} \tag{1.15}$$

The probability in the right hand side is given by

$$\begin{aligned} \boldsymbol{P}(Y \le p_r, Y \le N\gamma) &= \boldsymbol{P}(Y \le \min(p_r, N\gamma)) \\ &= \begin{cases} \int_{-\infty}^{p_r} f_Y(y)dy & \text{, if } p_r \le N\gamma \\ \int_{-\infty}^{N\gamma} f_Y(y)dy & \text{, otherwise} \end{cases} \end{aligned} \tag{1.16}$$

By differentiating with respect to p_r we obtain

$$f_{P,E_1|H_0}(p_r) = \begin{cases} f_Y(p_r) & \text{, if } p_r \leq N\gamma \\ 0 & \text{, otherwise} \end{cases} \tag{1.17}$$

The expression for Rayleigh fading is straightforward.

Case E_0**,** H_0

The PDF of P is now given by

$$\begin{aligned} f_{P,E_0|H_0}(p_r, E_0|H_1) &= \frac{\partial}{\partial p_r}\boldsymbol{P}\left(P \leq p_r, \mathtt{SINR} > \gamma | H_1\right) \\ &= \frac{\partial}{\partial p_r}\boldsymbol{P}\left(Y \leq p_r, Y > N\gamma\right) \end{aligned} \tag{1.18}$$

where $\boldsymbol{P}\left(Y \leq p_r, Y > N\gamma\right)$ equals $\boldsymbol{P}\left(N\gamma < Y \leq p_r\right)$ when $p_r > N\gamma$ and is 0 otherwise. Therefore we have

$$f_{P,E_0|H_0}(p_r) = \begin{cases} \dfrac{\partial}{\partial p_r}\displaystyle\int_{N\gamma}^{p_r} f_Y(y)dy & \text{, if } p_r > N\gamma \\ 0 & \text{, otherwise} \end{cases} \tag{1.19}$$

The particularization for Rayleigh fading is straightforward.

Given the above expressions, the MAP rule is specified by partitioning the observation space into disjoint sets in which each of the two hypothesis is chosen. In case a reception error has occurred (E_1), the following equation provides the threshold value(s) for the received power

$$\boldsymbol{P}(H_0)\, f_{P,E_1|H_0}(p_r) = \boldsymbol{P}(H_1)\, f_{P,E_1|H_1}(p_r) \tag{1.20}$$

And in the E_0 event, the corresponding equation is

$$\boldsymbol{P}(H_0)\, f_{P,E_0|H_0}(p_r) = \boldsymbol{P}(H_1)\, f_{P,E_0|H_1}(p_r) \tag{1.21}$$

Let us determine the power thresholds for the case of Rayleigh fading. Considering exponential distributions for X and Y in (1.20), we obtain the following two equations for E_1

$$lccl\boldsymbol{P}(H_0)\cdot 0 = \quad \boldsymbol{P}(H_1)\frac{e^{-\frac{p_r}{p_{ps}}} - e^{\left(-\frac{p_r}{p_{ss}} + \frac{(p_{ps}-p_{ss})(p_r-N\gamma)}{p_{ps}p_{ss}(1+\gamma)}\right)}}{p_{ps}-p_{ss}}, \text{if } p_r > N\gamma \tag{1.22}$$

$$\boldsymbol{P}(H_0)\frac{e^{-\frac{p_r}{p_{ss}}}}{p_{ss}} = \quad \boldsymbol{P}(H_1)\frac{e^{-\frac{p_r}{p_{ps}}} - e^{-\frac{p_r}{p_{ss}}}}{p_{ps}-p_{ss}}, \text{if } p_r \leq N\gamma \tag{1.23}$$

The first equation (1.22) only holds for $p_r = \infty$. Therefore, whenever $p_r > N\gamma$, the MAP rule selects the hypothesis H_1, which is rational because if $p_r > N\gamma$, the hypothesis H_0 implies that $\mathtt{SINR} > \gamma$ which is inconsistent with E_1. In other words, if $p_r > N\gamma$, E_1 is caused by PU interference. It can be checked that the solution of second equation (1.23) is

$$p^* = \frac{p_{ss}p_{ps}}{p_{ps} - p_{ss}} \log\left(\frac{p_{ps} - p_{ss}}{p_{ss}} \frac{\boldsymbol{P}(H_0)}{\boldsymbol{P}(H_1)} + 1\right) \tag{1.24}$$

If p^* is a real number and $p^* \leq N\gamma$, then $p^*_{E_1} = p^*$ is the threshold below which the MAP rule selects the hypothesis H_0 in the event E_1. In case (1.23) has no solution in $(0, N\gamma]$, then $p^*_{E_1} = N\gamma$ if the left hand side of (1.23) is larger than the right hand side, and $p^*_{E_1} = 0$ otherwise.

Considering Rayleigh fading, the equation for E_0, (1.21) results in the following two equations

$$lccl\boldsymbol{P}(H_0)\frac{e^{-\frac{p_r}{p_{ss}}}}{p_{ss}} = \boldsymbol{P}(H_1)\frac{e^{-\frac{p_r}{p_{ss}}}\left(e^{\frac{(p_{ps}-p_{ss})(p_r-N\gamma)}{p_{ps}p_{ss}(1+\gamma)}} - 1\right)}{p_{ps} - p_{ss}}, \text{if } p_r > N\gamma \tag{1.25}$$

$$\boldsymbol{P}(H_0)\cdot 0 = \boldsymbol{P}(H_1)\cdot 0, \text{if } p_r \leq N\gamma \tag{1.26}$$

The second equation (1.26) is trivially held for every $p_r \leq N\gamma$ because it corresponds to an unfeasible event: the absence of error when $p_r \leq N\gamma$ i.e. when $\texttt{SINR} \leq \gamma$. For $p_r > N\gamma$ equation (1.25) has the following solution

$$p^* = \frac{p_{ss}p_{ps}(1+\gamma)}{p_{ps} - p_{ss}}\left(\log\left(\frac{p_{ps} - p_{ss}}{p_{ss}} \frac{\boldsymbol{P}(H_0)}{\boldsymbol{P}(H_1)} + 1\right) + \frac{N\gamma(p_{ps} - p_{ss})}{p_{ss}p_{ps}(1+\gamma)}\right) \tag{1.27}$$

If p^* is a real number and $p^* > N\gamma$, then $p^*_{E_0} = p^*$ is the threshold above which the MAP rule selects the hypothesis H_1 in the event E_0. Otherwise one of the two hypothesis always holds. The threshold is defined as $p^*_{E_0} = N\gamma$ if H_1 always holds or as $p^*_{E_0} = \infty$ if H_0 always holds.

We have therefore determined four disjoint sets in the observation space:

$$lclR_{H_0E_0} = \left\{(p_r, e) : p_r \leq p^*_{E_0}, e = 0\right\} \tag{1.28}$$

$$R_{H_1E_0} = \left\{(p_r, e) : p_r > p^*_{E_0}, e = 0\right\} \tag{1.29}$$

$$R_{H_0E_1} = \left\{(p_r, e) : p_r \leq p^*_{E_1}, e = 1\right\} \tag{1.30}$$

$$R_{H_1E_1} = \left\{(p_r, e) : p_r > p^*_{E_1}, e = 1\right\} \tag{1.31}$$

When X and Y are not described by exponential distributions, the procedure to determine the $R_{H_iE_j}$ sets is analogous to the one described. These sets are not only useful to establish the MAP rule, but also to estimate the probabilities of correct or incorrect detection.

Detection Probability

For each possible combination of H_0, H_1 and E_0, E_1, two outcomes of the MAP estimation are possible, $\hat{H}_0$, $\hat{H}_1$, corresponding to the hypothesis $\hat{\theta} = 0$ and $\hat{\theta} = 1$ respectively. Selecting $\hat{H}_1$ when H_0 is true is generally referred to as a Type I error, and selecting $\hat{H}_0$ when H_1 is true is a Type II error.

Let us first consider the analysis of the probabilities for H_1, i.e. when transmission overlap is present. The probability of a Type II error when the SU packet is received correctly is defined as

$$\boldsymbol{P}(\hat{H}_0, E_0|H_1) = \boldsymbol{P}\left((P,E) \in R_{H_0E_0}|H_1\right), \tag{1.32}$$

the probability of correct PU activity detection when the SU packet is received correctly is

$$\boldsymbol{P}(\hat{H}_1, E_0|H_1) = \boldsymbol{P}\left((P,E) \in R_{H_1E_0}|H_1\right), \tag{1.33}$$

the Type II error probability when the SU packet received is erroneous is

$$\boldsymbol{P}(\hat{H}_0, E_1|H_1) = \boldsymbol{P}\left((P,E) \in R_{H_0E_1}|H_1\right), \tag{1.34}$$

and the probability of correct PU activity detection when the SU packet received is erroneous is

$$\boldsymbol{P}(\hat{H}_1, E_1|H_1) = \boldsymbol{P}\left((P,E) \in R_{H_1E_1}|H_1\right), \tag{1.35}$$

Let us obtain these probabilities for sets $R_{H_iE_j}$ defined with two thresholds ($p^*_{E_0}$ and $p^*_{E_1}$) and then particularize for Rayleigh fading. The probability $\boldsymbol{P}(\hat{H}_0, E_0|H_1)$ is given by

$$\begin{aligned}\boldsymbol{P}(\hat{H}_0, E_0|H_1) &= \boldsymbol{P}\left(P \le p^*_{E_0}, \mathtt{SINR} > \gamma|H_1\right)\\ &= \boldsymbol{P}\left(X+Y \le p^*_{E_0}, Y > N\gamma + X\gamma\right)\\ &= \boldsymbol{P}\left(N\gamma + X\gamma < Y \le p^*_{E_0} - X\right)\\ &= \int_0^{x^*}\int_{N\gamma+x\gamma}^{p^*_{E_0}-x} f_Y(y) f_X(x)\,dy\,dx\end{aligned} \tag{1.36}$$

where

$$x^* = \frac{p^*_{E_0} - N\gamma}{\gamma+1} \tag{1.37}$$

Solving for X and Y exponentially distributed we obtain the following probability

$$\boldsymbol{P}(\hat{H}_0, E_0|H_1) = e^{-\frac{x^*}{p_{ps}}} p_{ss} \frac{e^{\frac{p^*_{E_0}}{p_{ss}}}\left(e^{-\frac{x^*}{p_{ss}}} - e^{\frac{x^*}{p_{ps}}}\right)}{p_{ss}-p_{ps}} + \frac{e^{-\frac{((N+x^*)\gamma)}{p_{ss}}}\left(e^{x^*\left(\frac{1}{p_{ps}}+\frac{\gamma}{p_{ss}}\right)} - 1\right)}{p_{ss} - p_{ps}\gamma} \tag{1.38}$$

The probability of correct PU detection at the E_0 event is obtained as follows

$$\begin{aligned}\boldsymbol{P}(\hat{H}_1, E_0|H_1) &= \boldsymbol{P}\left(P > p^*_{E_0}, \mathtt{SINR} > \gamma|H_1\right)\\ &= \boldsymbol{P}\left(X+Y > p^*_{E_0}, Y > N\gamma + X\gamma\right)\\ &= \boldsymbol{P}\left(Y > \max\left(p^*_{E_0} - X, N\gamma + X\gamma\right)\right)\\ &= \int_0^{x^*}\int_{p^*_{E_0}-x\gamma}^{\infty} f_Y(y) f_X(x)\,dy\,dx + \int_{x^*}^{\infty}\int_{N\gamma+x\gamma}^{\infty} f_Y(y) f_X(x)\,dy\,dx\end{aligned} \tag{1.39}$$

The expression for Rayleigh fading is

$$\boldsymbol{P}(\hat{H}_1, E_0|H_1) = \frac{e^{-\frac{p^*_{E_0}}{p_{ss}}}\left(-1 + e^{\left(\frac{1}{p_{ss}} - \frac{1}{p_{ps}}\right)x^*}\right) p_{ss}}{p_{ps} - p_{ss}} + \frac{e^{-\frac{x^*}{p_{ss}} - \frac{\gamma(N+x^*)}{p_{ss}}} p_{ss}}{p_{ss} + p_{ps}\gamma} \tag{1.40}$$

The probability Type II error at the E_1 event is given by

$$\begin{aligned}
\boldsymbol{P}(\hat{H}_0, E_1|H_1) &= \boldsymbol{P}\left(P \leq p^*_{E_1}, \texttt{SINR} \leq \gamma|H_1\right) \\
&= \boldsymbol{P}\left(X+Y \leq p^*_{E_1}, Y \leq N\gamma + X\gamma\right) \\
&= \boldsymbol{P}\left(Y \leq \min\left(N\gamma + X\gamma, p^*_{E_1} - X\right)\right) \\
&= \boldsymbol{P}\left(Y \leq p^*_{E_1} - X\right) \\
&= \int_0^{p^*_{E_1}} \int_0^{p^*_{E_1}-x} f_Y(y) f_X(x) dy dx
\end{aligned} \tag{1.41}$$

where the last equality comes from the fact that $p^*_{E_1} \leq N\gamma$. The expression for Rayleigh fading is

$$\boldsymbol{P}(\hat{H}_0, E_1|H_1) = \frac{p_{ps}\left(1 - e^{-\frac{p^*_{E_1}}{p_{ps}}}\right) + \left(-1 + e^{-\frac{p^*_{E_1}}{p_{ss}}}\right) p_{ss}}{p_{ps} - p_{ss}} \tag{1.42}$$

The probability correct PU activity detection at E_1 is

$$\begin{aligned}
\boldsymbol{P}(\hat{H}_1, E_1|H_1) &= \boldsymbol{P}\left(P > p^*_{E_1}, \texttt{SINR} \leq \gamma|H_1\right) \\
&= \boldsymbol{P}\left(X+Y > p^*_{E_1}, Y \leq N\gamma + X\gamma\right) \\
&= \boldsymbol{P}\left(p^*_{E_1} - X < Y \leq N\gamma + X\gamma\right) \\
&= \int_0^{p^*_{E_1}} \int_{p^*_{E_1}-x}^{N\gamma+x\gamma} f_Y(y) f_X(x) dy dx + \int_{p^*_{E_1}}^{\infty} \int_0^{N\gamma+x\gamma} f_Y(y) f_X(x) dy dx
\end{aligned} \tag{1.43}$$

For Rayleigh fading the expression of this probability is

$$\boldsymbol{P}(\hat{H}_1, E_1|H_1) = \frac{e^{-\frac{p^*_{E_1}}{p_{ps}}} p_{ps}}{p_{ps} - p_{ss}} + \frac{e^{-\frac{p^*_{E_1}}{p_{ss}}} p_{ss}}{-p_{ps} + p_{ss}} - \frac{e^{-\frac{N\gamma}{p_{ss}}} p_{ss}}{p_{ss} + p_{ps}\gamma} \tag{1.44}$$

It can be checked that $\sum_{i:0,1} \sum_{j:0,1} \boldsymbol{P}(\hat{H}_i, E_j|H_1) = 1$. Figure 1.2 illustrates the integration regions for the detection probabilities under transmission overlap.

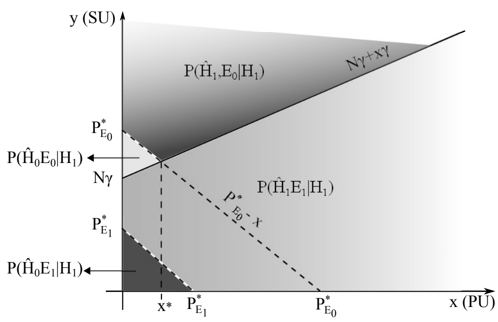

Figure 1.2: Integration regions to compute probabilities of correct detection, type I and type II errors under the H_1 event (transmission overlap).

Let us now obtain the probabilities for H_0, i.e. in absence of transmission overlap. The probabilities are defined in the following way

$$lcl\boldsymbol{P}(\hat{H}_0, E_0|H_0) = \boldsymbol{P}\left((P,E) \in R_{H_0E_0}|H_0\right) \tag{1.45}$$
$$\boldsymbol{P}(\hat{H}_1, E_0|H_0) = \boldsymbol{P}\left((P,E) \in R_{H_1E_0}|H_0\right) \tag{1.46}$$
$$\boldsymbol{P}(\hat{H}_0, E_1|H_0) = \boldsymbol{P}\left((P,E) \in R_{H_0E_1}|H_0\right) \tag{1.47}$$
$$\boldsymbol{P}(\hat{H}_1, E_1|H_0) = \boldsymbol{P}\left((P,E) \in R_{H_0E_1}|H_0\right) \tag{1.48}$$

We now obtain these probabilities as in the H_1 case. The correct estimation probability $\boldsymbol{P}(\hat{H}_0, E_0|H_0)$ is given by

$$\begin{aligned}\boldsymbol{P}(\hat{H}_0, E_0|H_0) &= \boldsymbol{P}\left(P \leq p^*_{E_0}, \mathtt{SINR} > \gamma|H_0\right) \\ &= \boldsymbol{P}\left(Y \leq p^*_{E_0}, Y > N\gamma\right) \\ &= \boldsymbol{P}\left(N\gamma < Y \leq p^*_{E_0}\right) \\ &= \int_{N\gamma}^{p^*_{E_0}} f_Y(y)dy\end{aligned} \tag{1.49}$$

which, in the case of Rayleigh fading equals $e^{-N\gamma/p_{ss}} - e^{-p^*_{E_0}/p_{ss}}$. The Type I error $\boldsymbol{P}(\hat{H}_0, E_0|H_0)$ is

$$\begin{aligned}\boldsymbol{P}(\hat{H}_1, E_0|H_0) &= \boldsymbol{P}\left(P > p^*_{E_0}, \mathtt{SINR} > \gamma|H_0\right) \\ &= \boldsymbol{P}\left(Y > p^*_{E_0}, Y > N\gamma\right) \\ &= \boldsymbol{P}\left(Y > \max\left(p^*_{E_0}, N\gamma\right)\right) \\ &= \boldsymbol{P}\left(Y > p^*_{E_0}\right) \\ &= \int_{p^*_{E_0}}^{\infty} f_Y(y)dy\end{aligned} \tag{1.50}$$

For Rayleigh fading $\boldsymbol{P}(\hat{H}_1, E_0|H_0) = e^{-p^*_{E_0}/p_{ss}}$. The correct estimation probability at the E_1 event is

$$\begin{aligned}\boldsymbol{P}(\hat{H}_0, E_1|H_0) &= \boldsymbol{P}\left(P \leq p^*_{E_1}, \mathtt{SINR} \leq \gamma|H_0\right) \\ &= \boldsymbol{P}\left(Y \leq p^*_{E_1}, Y \leq N\gamma\right) \\ &= \boldsymbol{P}\left(Y \leq \min\left(N\gamma + X\gamma, p^*_{E_1}\right)\right) \\ &= \boldsymbol{P}\left(Y \leq p^*_{E_1}\right) \\ &= \int_{0}^{p^*_{E_1}} f_Y(y)dy\end{aligned} \tag{1.51}$$

which for Rayleigh fading is $1 - e^{-p^*_{E_1}/p_{ss}}$. Finally the Type I error probability at the E_1 event is

$$\begin{aligned}\boldsymbol{P}(\hat{H}_1, E_1|H_0) &= \boldsymbol{P}\left(P > p^*_{E_1}, \mathtt{SINR} \leq \gamma|H_0\right) \\ &= \boldsymbol{P}\left(Y > p^*_{E_1}, Y \leq N\gamma\right) \\ &= \boldsymbol{P}\left(p^*_{E_1} < Y \leq N\gamma\right) \\ &= \int_{p^*_{E_1}}^{N\gamma} f_Y(y)dy\end{aligned} \tag{1.52}$$

which equals $e^{-p^*_{E_1}/p_{ss}} - e^{-N\gamma/p_{ss}}$ for Rayleigh fading.

1.4 Markov Model for Optimized OSA

In this section, we analyze the use of the proposed background detection (BD) mechanism in an OSA system maximizing the SU throughput subject to constraints on the collision probability with PU transmissions. We assume single-channel transmission capabilities for the SU, leaving for future research the generalization to the multiple-channel case. An SU transmission period consists of one scanning slot followed by N consecutive time-slots. The SU detects at least one available channel during the scanning slot, otherwise this scanning slot does not corresponds to a scanning slot. After the scanning slot, the SU transmits one data packet in each one of the N remaining time-slots of the SU transmission period. Note that N denotes, in general, a random variable. However, as later explained, this is only the case for OSA with BD. Two parameters characterize the system performance: the SU throughput (T), defined as the expected number of correctly received SU packets per time-slot in an SU transmission period, and the collision probability P_c, defined as the PU-SU transmission overlap probability per time-slot in a SU transmission period.

PU inter arrival time follows a geometric distribution as well as the channel holding time, i.e. the equivalent of a Poisson traffic model for discrete-time. In every time-slot, a channel free of PU traffic is occupied by a PU transmission with probability p, and an ongoing PU transmission ends with probability q. The SU uses estimations of p and q to optimize the duration of the transmission period under collision probability constraints. The effect that the estimation inaccuracies in both the traffic intensity and in the traffic model have in the OSA performance is addressed in Section 1.5.

Considering the n-th time-slot of an SU transmission period, ϕ_n denotes the probability vector for PU activity in the channel during this time-slot. In the single-channel traffic model considered, ϕ_n contains two elements: $\phi_n(1)$ and $\phi_n(2)$, corresponding to no PU activity and PU activity in the channel respectively. The probability vector in the scanning slot is $\phi_0 = (1, 0)$ if the detection is perfect. With imperfect sensing, $\phi_0 = (1 - p_{\bar{n}}, p_{\bar{n}})$, where $p_{\bar{n}}$ denotes the probability of false negative (the sensing outcome indicates that the channel is free of PU activity when it is not). Given the transition matrix of the Markov model for the PU activity in the channel, $M = \left[\begin{smallmatrix} 1-p & p \\ q & 1-q \end{smallmatrix}\right]$, the probability vector for the n-th time-slot is given by $\phi'_n = M^n \phi'_n$, where "$'$" stands for the transpose operation.

OSA Without Background Detection

In this case, after the scanning slot, the SU transmits in the channel during a fixed number of slots. In an optimized OSA, this number maximizes T while P_c remains below a given value α. Let $T(n)$ and $P_c(n)$ denote T and P_c as functions of n. The optimized OSA selects a number of time-slots solving the following problem

$$\max_{n} T(n) \text{ subject to } P_c(n) \leq \alpha \tag{1.53}$$

which is solved for nonnegative integers n up to a maximum value n_{m}, which stands for avoiding unbounded n in case $T(n)$ attains its maximum at $n \to \infty$ and $P_c(n)$

remains under α for every n. Note that, provided that $\phi_0 = (1,0)$, $P_c(n)$ is a monotonically increasing sequence bounded by $p/(p+q)$. If several values of n attain the maximum, the OSA algorithm picks the one with the lowest P_c. We refer to this value as n^*.

The expression for $P_c(n)$ is given by

$$P_c(n) = \frac{1}{n+1}\sum_{i=1}^{n}\phi_i(2) \tag{1.54}$$

Defining $\boldsymbol{P}(E_0|H_0)$ as the probability of correctly receiving an SU packet in the absence of collision, and $\boldsymbol{P}(E_0|H_1)$ as the probability of E_0 in a time-slot with collision, $T(n)$ is given by the following equation

$$T(n) = \frac{1}{n+1}\left[\sum_{i=1}^{n}\phi_i(1)\boldsymbol{P}(E_0|H_0) + \sum_{i=1}^{n}\phi_i(2)\boldsymbol{P}(E_0|H_1)\right] \tag{1.55}$$

The probability $\boldsymbol{P}(E_0|H_0)$ is obtained as follows

$$\begin{aligned} \boldsymbol{P}(E_0|H_0) &= \boldsymbol{P}\left(\mathtt{SINR} > \gamma|H_0\right) \\ &= \boldsymbol{P}\left(Y > N\gamma\right) \\ &= \int_{N\gamma}^{\infty} f_Y(y)dy \end{aligned} \tag{1.56}$$

and $\boldsymbol{P}(E_0|H_1)$ is given by

$$\begin{aligned} \boldsymbol{P}(E_0|H_1) &= \boldsymbol{P}\left(\mathtt{SINR} > \gamma|H_1\right) \\ &= \boldsymbol{P}\left(Y > N\gamma + X\gamma\right) \\ &= \int_{0}^{\infty}\int_{N\gamma+x\gamma}^{\infty} f_Y(y)f_X(x)dydx \end{aligned} \tag{1.57}$$

For Rayleigh fading we have

$$lcl\boldsymbol{P}(E_0|H_0) = e^{-\frac{N\gamma}{p_{ss}}} \tag{1.58}$$

$$\boldsymbol{P}(E_0|H_1) = \frac{p_{ss}e^{-\frac{N\gamma}{p_{ss}}}}{p_{ss}+p_{ps}\gamma} \tag{1.59}$$

OSA With Background Detection

In contrast to previous scheme, when OSA includes BD, the duration of the SU transmission period is not deterministic. Because BD can detect PU activity simultaneously to SU packet reception, the SU transmission can be aborted at any time-slot. Figure 1.3 compares a transmission period without BD with two possible outcomes of the transmission period using BD. Case (a) is the standard SU transmission period when the BD scheme does not detect PU activity in any slot. Case (b) corresponds to the case when the BD scheme detects a PU transmission is a slot, resulting in the immediate termination of the SU transmission in this channel.

In order to compute T and P_c we develop a Markov-reward model of the SU transmission process, consisting in a discrete-time Markov chain (DTMC) in which

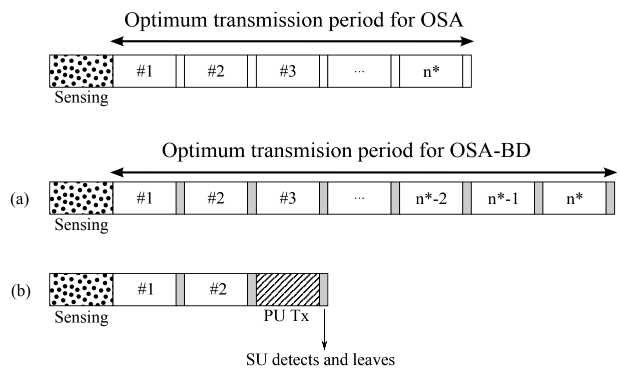

Figure 1.3: Transmission periods with and without BD. When using BD the transmission period can be aborted if PU activity is detected during an SU transmission slot. Inter-slot periods are required for signaling.

each state is associated to a reward defined in terms of T of P_c, depending on what is being computed. The DTMC, denoted by Z_k, characterizes a process of consecutive SU transmissions, where k enumerates time-slots. The integer value i taken by Z_k. i.e. the state of the DTMC at the k-th time-slot, has the following interpretation:

- If i is odd, the channel is free of PU activity (H_0) at the $\lceil i/2 \rceil$-th time-slot.
- If i is even, the channel presents PU activity (H_1) at the $i/2$-th time-slot.

After the scanning time-slot ($i = 0$), the SU transmits with probability 1, and enters state $i = 1$ with probability $1 - p$ and state $i = 2$ with probability p. The DTMC advances to a higher state if the BD does not detect PU activity ($\hat{H}_0$), and returns to state 0 otherwise, which means the end of the ongoing SU transmission. Therefore, the DTMC transition probabilities are defined as

$$\begin{array}{lcll} p_{0,1} & = & 1-p & \\ p_{0,2} & = & p & \\ p_{2k-1,2k+1} & = & (1-p)\boldsymbol{P}(\hat{H}_0|H_0) & , \text{ for } 0<k<n \\ p_{2k-1,2k+2} & = & p\boldsymbol{P}(\hat{H}_0|H_0) & , \text{ for } 0<k<n \\ p_{2k-1,0} & = & 1-\boldsymbol{P}(\hat{H}_0|H_0) & , \text{ for } 0<k<n \\ p_{2k,2k+1} & = & q\boldsymbol{P}(\hat{H}_0|H_1) & , \text{ for } 0<k<n \\ p_{2k,2k+2} & = & (1-q)\boldsymbol{P}(\hat{H}_0|H_1) & , \text{ for } 0<k<n \\ p_{2k,0} & = & 1-\boldsymbol{P}(\hat{H}_0|H_1) & , \text{ for } 0<k<n \\ p_{n,0} & = & 1 & \end{array} \tag{1.60}$$

where $\boldsymbol{P}(\hat{H}_0|H_0)$ and $\boldsymbol{P}(\hat{H}_0|H_1)$ can be obtained as follows

$$\begin{aligned}\boldsymbol{P}(\hat{H}_0|H_0) &= \boldsymbol{P}(\hat{H}_0, E_0|H_0) + \boldsymbol{P}(\hat{H}_0, E_1|H_0)\\ \boldsymbol{P}(\hat{H}_0|H_1) &= \boldsymbol{P}(\hat{H}_0, E_0|H_1) + \boldsymbol{P}(\hat{H}_0, E_1|H_1)\end{aligned} \tag{1.61}$$

where $\boldsymbol{P}(\hat{H}_0, E_0|H_1)$, $\boldsymbol{P}(\hat{H}_0, E_1|H_1)$, $\boldsymbol{P}(\hat{H}_0, E_0|H_0)$, and $\boldsymbol{P}(\hat{H}_0, E_1|H_0)$, are obtained by (1.36), (1.41), (1.49), and (1.51)respectively. Figure 1.4 depicts the graph of the DTMC.

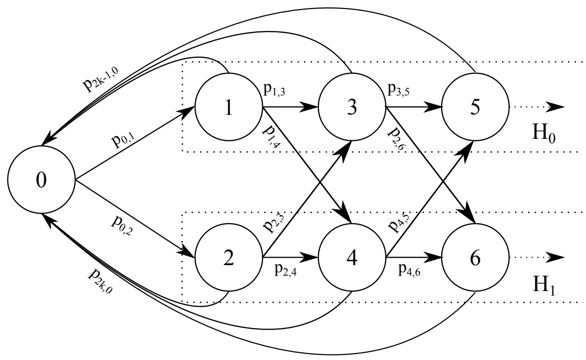

Figure 1.4: Graph of the DTMC characterizing the SU transmission process.

For a generic reward $r(i)$, the expected average reward is defined as $\bar{r} = \lim_{K\to\infty} \frac{1}{K}\sum_{k=0}^{K} r(Z_k)$. For an ergodic, finite-state Markov chain, and provided that $|r(i)|$ is bounded for every i, the total expected average reward $\bar{r}$ is $\bar{r} = \sum_{i=0}^{n} r(i)\,\pi_i$, where π_i are the steady state probabilities of the DTMC obtained by solving the equilibrium equations $\boldsymbol{\pi} = \boldsymbol{\pi T}$, $\|\boldsymbol{\pi}\| = \displaystyle\sum_{i=0}^{n} \pi_i = 1$, where $\boldsymbol{T}$ is the transition matrix containing the probabilities defined in (1.60). Let $r_T(i)$ and $r_{P_c}(i)$ denote the per-state reward for computing T and P_c respectively. According to the definitions of T and P_c, and because the DTMC models consecutive SU transmissions, $\bar{r}_T = T$ and $\bar{r}_{P_c} = P_c$. We will use the terms $\bar{r}_T(n)$ and $\bar{r}_{P_c}(n)$ to refer to the SU throughput and collision probability when using BD and the maximum length of SU transmissions is set to n time-slots. The optimal n is obtained by solving the following optimization problem

$$\max_{n} \bar{r}_T(n) \text{ subject to } \bar{r}_{P_c}(n) \leq \alpha \tag{1.62}$$

which is solved for integers $n \in \{0, 1, \ldots, n_{\mathrm{m}}\}$. Note that the trivial values for $n = 0$ are $\bar{r}_T(0) = 0$ and $\bar{r}_{P_c}(0) = 0$. If there are more than one solution, the optimal transmission limit n^* is the lowest one attaining the maximum throughput.

Let us see how to obtain $r_T(i)$ and $r_{P_c}(i)$ for every i. The per-stage throughput $r_T(i)$ is defined as the expected number of SU packets correctly received at the i-th SU transmission time-slot. By definition, for every $i > 0$, the SU transmits one packet, therefore $r_T(i) = \boldsymbol{P}(E_0|i)\cdot 1$, where $\boldsymbol{P}(E_0|i)$ is the probability of the E_0 event at the i-th time-slot, and is given by

$$\boldsymbol{P}(E_0|i) = \begin{cases}\boldsymbol{P}(E_0|H_0) & \text{, if } i \text{ odd}\\ \boldsymbol{P}(E_0|H_1) & \text{, if } i \text{ even}\end{cases} \tag{1.63}$$

for $i > 0$, where $\boldsymbol{P}(E_0|H_0)$ and $\boldsymbol{P}(E_0|H_1)$ are given by (1.56) and (1.57) respectively. Similarly, the per-stage collision probability is $r_{P_c}(i) = 0$ when i is odd, and $r_{P_c}(i) = 1$ when i is even. For $i = 0$ we have $r_T(0) = 0$ and $r_{P_c}(0) = 0$.

The specific structure of matrix $\boldsymbol{T}$ allows an efficient computation of the steady-state probability vector $\boldsymbol{\pi}$. Let us express $\boldsymbol{T}$ in a block-matrix form

$$\boldsymbol{T} = \begin{pmatrix} \mathbf{B}_{0,0} & \mathbf{B}_{0,1} & \mathbf{0} & \mathbf{0} & \cdots \mathbf{0} \\ \mathbf{B} & \mathbf{0} & \mathbf{A} & \mathbf{0} & \cdots \mathbf{0} \\ \mathbf{B} & \mathbf{0} & \mathbf{0} & \mathbf{A} & \cdots \mathbf{0} \\ \vdots & \vdots & \vdots & \vdots & \vdots \\ \mathbf{1} & \mathbf{0} & \mathbf{0} & \mathbf{0} & \cdots \mathbf{A} \end{pmatrix} \tag{1.64}$$

where $\mathbf{B}_{0,0} = (0, 0)$, $\mathbf{B}_{0,1} = ((1-p), p)$, and

$$\begin{aligned} \boldsymbol{A} &= \begin{pmatrix} (1-p)\boldsymbol{P}(\hat{H}_0|H_0) & p\boldsymbol{P}(\hat{H}_0|H_0) \\ q\boldsymbol{P}(\hat{H}_0|H_1) & (1-q)\boldsymbol{P}(\hat{H}_0|H_1) \end{pmatrix} \\ \boldsymbol{B} &= \begin{pmatrix} 1-\boldsymbol{P}(\hat{H}_0|H_0) \\ 1-\boldsymbol{P}(\hat{H}_0|H_1) \end{pmatrix} \\ \mathbf{1} &= \begin{pmatrix} 1 \\ 1 \end{pmatrix} \end{aligned} \tag{1.65}$$

Let us define $\boldsymbol{\pi}_k = (\pi_{2k-1}, \pi_{2k})$, denoting the probability of the events H_0 and H_1 at the k-th transmission slot. Applying the equilibrium equations we have $\pi_0 = \sum_{k=1}^{n-1} \boldsymbol{\pi}_j \mathbf{B} + \boldsymbol{\pi}_n \mathbf{1}$, $\boldsymbol{\pi}_1 = \pi_0 \mathbf{B}_{0,1}$, and $\boldsymbol{\pi}_k$ can be expressed in the matrix-geometric form $\boldsymbol{\pi}_k = \boldsymbol{\pi}_1 \boldsymbol{A}^{k-1} = \pi_0 \mathbf{B}_{0,1} \boldsymbol{A}^{k-1}$. The normalization condition is $\pi_0 + \sum_{k=1}^{n-1} \boldsymbol{\pi}_j \mathbf{1} + \boldsymbol{\pi}_n \mathbf{1} = 1$, which combined with the equilibrium equations results in the following expression for π_0

$$\pi_0 = \frac{1}{2 + \sum_{k=1}^{n-1} \mathbf{B}_{0,1} \boldsymbol{A}^{k-1} (\mathbf{1} - \mathbf{B})} \tag{1.66}$$

Because $\boldsymbol{A}$ is strictly positive we know, by the Perron-Frobenius theorem, that it has one positive eigenvalue, with multiplicity 1, which is strictly higher than all other eigenvalues. Since the dimension of $\boldsymbol{A}$ is 2×2, it has only two eigenvalues and thus we conclude that $\boldsymbol{A}$ has two distinct eigenvalues, λ_1 and λ_2 (with their corresponding eigenvectors $\boldsymbol{e}_1$ and $\boldsymbol{e}_2$). This implies that $\boldsymbol{A}$ can be expressed as $\boldsymbol{A} = \boldsymbol{M} \Lambda \boldsymbol{M}^{-1}$ where $\boldsymbol{M} = [\boldsymbol{e}_1 \boldsymbol{e}_2]$ and Λ is a diagonal matrix containing (λ_1, λ_2) in its diagonal. Then

$$\boldsymbol{A}^{k-1} = \boldsymbol{M} \begin{pmatrix} \lambda_1^{k-1} & 0 \\ 0 & \lambda_2^{k-1} \end{pmatrix} \boldsymbol{M}^{-1} \tag{1.67}$$

which allows us to express (1.66) in the following closed form

$$\pi_0 = \left(2 + \mathbf{B}_{0,1} \boldsymbol{M} \begin{pmatrix} \frac{1-\lambda_1^{n-1}}{1-\lambda_1} & 0 \\ 0 & \frac{1-\lambda_2^{n-1}}{1-\lambda_2} \end{pmatrix} \boldsymbol{M}^{-1} (\mathbf{1} - \mathbf{B}) \right)^{-1} \tag{1.68}$$

which enables an efficient computation of $\boldsymbol{\pi}_k = \pi_0 \mathbf{B}_{0,1} \boldsymbol{A}^{k-1}$, for $k = 1, \ldots, n$.

Parameter	Assigned value
p_{ss}	-72.9 dBm
p_{ps}	-70.5 dBm
N	-103 dBm
γ	7 dBm
p	10^{-3}
q	$2 \cdot 10^{-3}$
$\boldsymbol{P}(H_1)$	1/3
$p^*_{E_0}$	-61.8 dBm
$p^*_{E_1}$	-95.9 dBm
$\boldsymbol{P}(\hat{H}_1 \vert H_0)$	$2.65 \cdot 10^{-6}$
$\boldsymbol{P}(\hat{H}_0 \vert H_1)$	0.1026

Table 1.1: Parameter setting of the reference scenario used in numerical evaluations

1.5 Numerical Results

Parameter Setting

To assess the impact of using BD on the performance and, especially, on the robustness of the OSA scheme, we consider a cognitive pair located within PU BS cell. The distance between the of PU BS and the SU Rx is $d_{ps} = 1000$ m. The PU BS transmission power on each channel, p_p, is 20 dBm. The transmission antenna height is $h_t = 10$ m and the receiver is at $h_r = 1.5$ m. The transmission and reception antenna gains are $g_t = 4$ dB and $g_r = 2$ dB respectively. With these parameters, the average interference power at the SU receiver due to PU BS transmission is given by the pathloss equation

$$p_{ps} = \frac{p_p (h_t h_r)^2 g_t g_r}{d_{ps}^{-4}} \tag{1.69}$$

which equals -70.5 dBm. Assuming that the SU Tx antenna height and gain are 1.5 m and 4 dB respectively and that the distance between SU Tx and the SU Rx is $d_{ss} = 250$ m, we obtain $p_{ss} = -72.9$ dBm. Considering a channel bandwidth $B = 2$ MHz, and an SU Rx noise figure equal to 18 dB, the total noise power is $N = -103$ dBm. The cognitive pair transmits at a rate of 2 Mbit/s using BPSK modulation and, as explained in Section 1.2, each packet is assumed to arrive correctly if BER$< 10^{-3}$, therefore the SINR threshold is $\gamma = 7$ dB. The PU traffic parameters are $p = 10^{-3}$ and $q = 2 \cdot 10^{-3}$, resulting in an occupation probability $\boldsymbol{P}(H_1) = \frac{1}{3}$. With these parameters we obtain the following thresholds for Rayleigh fading: $p^*_{E_0} = -61.8$ dBm and $p^*_{E_1} = -95.9$ dBm. The type I and type II error probabilities are $\boldsymbol{P}(\hat{H}_1|H_0) = 2.65 \cdot 10^{-6}$ and $\boldsymbol{P}(\hat{H}_0|H_1) = 0.1026$ respectively. The main parameters are summarized in Table 1.1.

Before evaluating the performance and robustness of optimally configured OSA with and without BD, it is interesting to assess how the performance parameters (throughput T and collision probability P_c) vary with the optimization parameter n (in time-slots). Figure 1.5 shows the throughput and collision performance versus n for both implementations. The values of T and P_c are obtained numerically and by simulation also, to validate the model. We can appreciate one of the main advantages of using BD: while P_c increases almost linearly with n when BD is not used, it does not surpass a notably low level when BD is used. The reason is that PU activity can be detected during SU transmission, implying the end of the transmission. Therefore, although n determines the maximum duration of a SU transmission when BD is used, the expected duration is determined by the PU activity detection. When BD is not used, larger values of n imply higher P_c and lower T, because transmission overlap also degrades SU performance. Seeing this figure, one can anticipate that the BD implementation may be more robust against parameter estimation inaccuracies, than the one without BD.

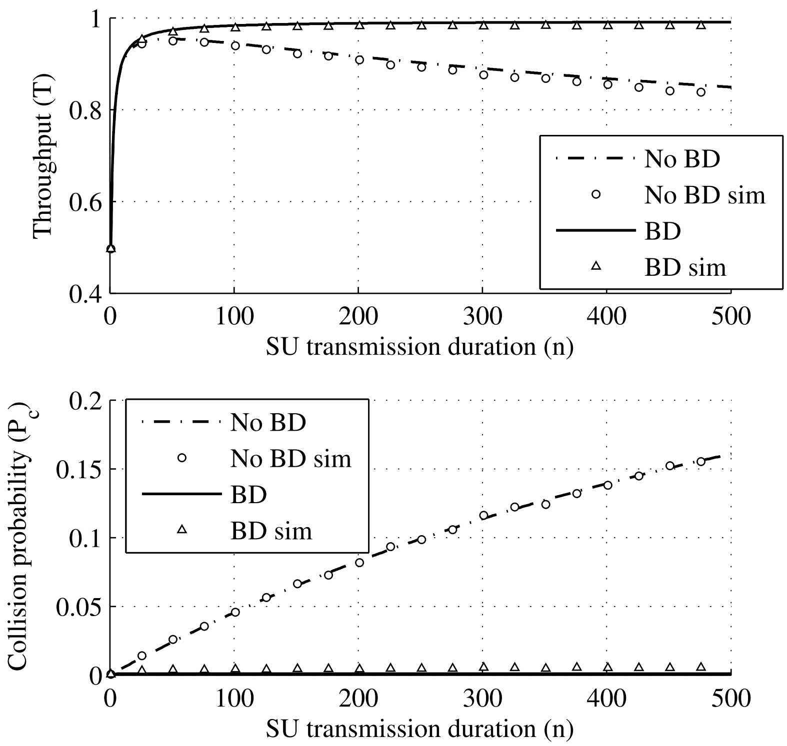

Figure 1.5: Throughput and collision performance with and without BS vs. the number of time-slots (n) of the SU transmission

Sensitivity to Estimation Inaccuracies

In this subsection we study how the optimized implementations of OSA and OSA with BD perform under drifts of the real values of some critical parameters. By doing this, we evaluate the robustness of each implementation against inaccuracies on the parameter estimation. With the parameters described in previous subsection, and setting the collision probability threshold $\alpha = 0.025$, the optimal n value for OSA without BD is 49. With BD, $T(n)$ increases monotonically with n, while $P(n)$

remains below 0.025. In this case we select $n = 100$ which provides a throughput very close to the maximum, and would result in, at most, 0.05 collision probability in case of a complete malfunction of th BD mechanism.

Both schemes are heavily reliant on the characterization of the PU traffic in the channel. To evaluate the impact of traffic estimation inaccuracies, let us consider that the arrival traffic intensity p differs from the estimated one p_{est}, which is used for the computation of n^* in both schemes and for the threshold computation in BD. Figure 1.6 shows the performance versus the ratio p/p_{est}. We see that in both cases, the T decreases and P_c increases but, for the BD case the degradation is notably less severe than the no BD case, showing the higher robustness of BD against error in traffic estimation.

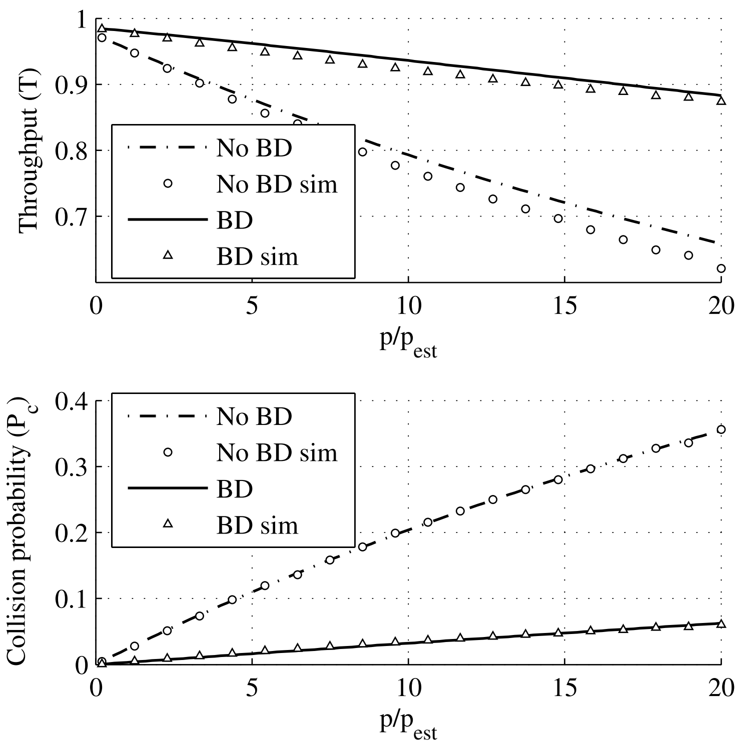

Figure 1.6: Throughput and collision performance with and without BS vs. the inaccuracy on the estimation of the traffic intensity

Another critical aspect in the BD scheme is the channel characterization. In the example developed, The MAP estimator is designed for a Rayleigh fading model for both PU and SU signals, assuming a previous knowledge of the average signal powers at the receiver. However it is possible that the SU misestimates the average power, especially for the PU signal (p_{ps}), or even the channel statistical description itself. To assess the effect of these misestimations, we have simulated an OSA system with BD configured for Rayleigh fading, to obtain the performance under different p_{ps} estimation errors when the fading is Rayleigh, Ricean with $K = 10$, and Nakagami with $m = 2$. We also compare these results with the performance of an OSA system without BD in the same scenarios. As can be seen in Figure 1.7, OSA with BD maintains its advantage respect to the non BD system in almost every case. The statistical characterization of the fading shows a moderate impact on BD performance. In contrast, overestimating p_{ps} shows to have the most harmful effect on the collision probability. The reason is that as the real p_{ps} decreases respect the estimated value, the probability of Type II error approaches 1 and, in consequence the OSA with BD tends to operate as an OSA without BD. In Figure 1.7, OSA BD is set to $n = 100$ which, as explained previously, results in a P_c near 0.05 in case of BD malfunctioning. If OSA and OSA BD are both configured with the same n value, they present similar performance under p_{ps} overestimation in the scenarios of Figure 1.7.

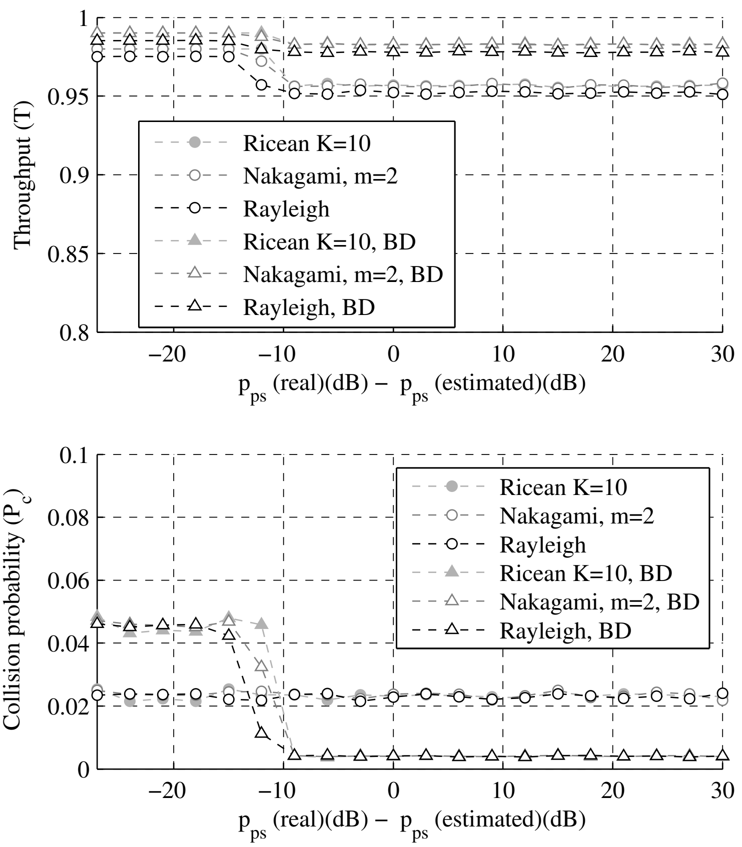

Figure 1.7: Throughput and collision performance with and without BS vs. the inaccuracy on the estimation of the traffic intensity

1.6 Conclusions

CHAPTER 2

Response Surface Methodology for Efficient Spectrum Reuse in Cellular Networks

2.1 Introduction

In this chapter we move on from mechanisms that ensure the proper operation of opportunistic access to develop a full DSA framework particularized for cellular networks.

Approximately every decade, a new cellular access technology is developed and introduced in the market. However, because not all users upgrade their terminals at the same pace, the operators have to keep their legacy networks working, and the spectrum assigned to these old networks becomes gradually more and more underused.

One way to increase the spectrum efficiency is to allow the users of the newest networks to opportunistically access the spectrum of the legacy networks. Applying the concepts of cognitive radio [174], the terminals of the newest network would be the secondary users (SUs), and the terminals of the legacy network would be the primary users (PUs). The secondary access to the spectrum of the primary (legacy) network should not cause noticeable degradation to PU transmissions.

The operator owns and control both the primary and the secondary networks, and therefore can establish the rules for secondary access and monitor the impact of these rules on the performance of both SU and PU transmissions. However, it is more profitable for the operator *not making any modifications on the legacy network*, implying that the operation of the secondary network is *transparent* to the primary network.

In this chapter, we propose a semi-decentralized secondary access scheme allowing each SU to access a set of primary frequency bands using either temporal or spatial spectrum holes (opportunities). By giving more access options to each SU, this approach can outperform previous, more limited, mechanisms. We consider that the SUs establish point-to-point connections among them (cognitive pairs) in an ad-hoc fashion.

To fully exploit its potential, we describe an on-line algorithm that, with very small computational and signaling overhead, allows the system to learn the optimal SU access policy in terms of capacity.

Related Work

Other works have proposed the combination of temporal and spatial sensing by the SUs [175], [176], [177], [178]. Works like [175] and [176] consider a single secondary transmitter and exploit information from spatial sensing to improve the performance of temporal sensing. The single transmitter model is also applied in [177] for vehicular networks. In [178] the capacity is optimized by randomizing the access strategies, but for a single PU, single SU scenario. However, the motivational scenario of our work comprises multiple secondary transmitters with multiple primary base stations. Thus, we must consider relevant features that are not captured by the single transmitter model, such as the inter-SU interference and the frequency reuse in a cellular structure.

In cellular networks, previous works like [179] and [180] have addressed spatial spectrum reuse by a secondary network. However, these works assume that the secondary users only scan one frequency. As pointed out by their authors, scanning all the frequencies would improve the performance. In contrast, we follow this latter approach, mixing it with the exploitation of temporal opportunities.

Contribution

Our contribution in this chapter is summarized as follows:

- We develop a semi-distributed mechanism for opportunistic spectrum access combining access over temporal and spatial opportunities, in which *all the spectrum of the system can be made available to each SU.*

- Our method is especially conceived for cellular networks, considering multiple PU transmitters within a cell structure. The system is evaluated in a realistic setting considering irregular cell shapes.

- The most important feature, 3) *the system is capable of learning the optimal probability distribution over the frequency bands of the cellular network* to maximize SU capacity. The learning algorithm applies the response surface methodology (RSM) [183], which is a novel and promising approach to address interference management problems.

In the following section we describe the system. Section 2.3 formulates the design problem and Section 2.4 presents the RSM algorithm to solve it. Finally, Sections 2.5 and 2.6 presents the numerical results and the conclusions of this work.

2.2 System description

The system considered comprises: a legacy cellular network (primary network), a secondary network establishing ad-hoc point-to-point links, and a secondary access controller (SAC) which monitors the system performance and broadcasts the operation parameters of the SU access strategy, with small signaling overhead, as we discuss in Section 2.4. The primary network contains base stations (PBSs) and primary users (PUs). Each PBS covers a certain geographical area (primary cell) and is assigned a frequency band different from its adjacent cells.

We assume a frequency reuse scheme of 7 frequency bands (reuse factor 7), denoted by $f_1, \ldots, f_7$. Nevertheless, the proposed method can be applied to other reuse factors as well. Each frequency band is divided into $2N$ orthogonal channels (N downlink and N uplink channels). Secondary access is constrained to downlink channels. Time is divided into equal duration time-slots, which is usual in most cellular systems. The data transmitted over a single PU channel in a time-slot is referred to as *packet*.

The secondary network consists of pairs of secondary users (SUs) entering and leaving the system in an ad-hoc fashion. This network model can characterize femtocells, terminals acting as relays, or any short-range transmission using available spectral resources of the legacy cellular network.

The SAC is associated to the network to which the SUs belong. In particular, we assume that the SUs are the users of a new generation cellular network. Because both networks (the new generation network and the legacy one) belong to the same operator, we consider that the SAC can retrieve some information from the legacy network.

The SUs can detect the power of the pilot tones of the neighboring PBSs. With this information (and possibly with the aid of the SAC) each SU can infer its position with respect to the surrounding cells and therefore be aware of the PBS power levels from each frequency band. Indeed, the SU does not need to estimate exactly these PBS power levels, it just needs to establish an ordering of the frequencies $f_1, \ldots, f_7$ from lower to higher PBS power level. For a generic SU, let $\boldsymbol{\phi} = (\phi_1, \ldots, \phi_7)$ be the vector of frequencies ordered in increasing received power, which clearly depends on the location of the SU. Note that ϕ_7 corresponds, in general, to the frequency band of the primary cell where the SU is located.

Example. In Figure 2.1, any SU located in area A has $\phi_1 = f_1$ (similarly, any SU in area B has $\phi_1 = f_2$). But because each SU is closer to a different PBS, $\phi_7 = f_5$ for SU 1, and $\phi_7 = f_6$ for SU 2. These SUs have also different values of ϕ_2 and ϕ_4.

When an SU transmits over any band ϕ_i, it may cause some interference to the PUs of the closest cells using this band (and the same channel within this band). In general, the level of SU interference caused at PU receivers is proportional to the ordering index i of the selected band ϕ_i, *i.e.* a single SU transmission over ϕ_1 causes generally less interference than an SU transmission over ϕ_2, and so on.

In our system, the classic strategy of occupying exclusively *spatial opportunities* implies that each SU only tries to access over ϕ_1. However, what really matters

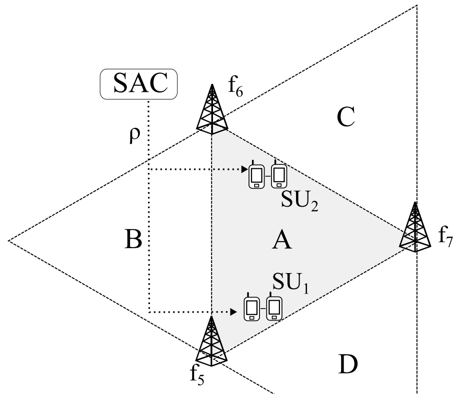

	ϕ_1	ϕ_2	ϕ_3	ϕ_4	ϕ_5	ϕ_6	ϕ_7
SU_1	f_1	f_4	f_2	f_3	f_6	f_7	f_5
SU_2	f_1	f_3	f_2	f_4	f_5	f_7	f_6

Figure 2.1: Example of the system with 2 SU pairs. Every SU in area A associates f_1 to ϕ_1. The remaining f_j-ϕ_i associations for each SU depend on how close the SU is to areas B, C or D. The SAC broadcasts a vector of operation parameters $\boldsymbol{\rho}$ to the SUs.

is the aggregate interference at the receivers. Note that, in accordance to the ad-hoc nature of the secondary network (small SU transmission range, low antenna heights, indoor locations sometimes) the SINR at the PU receivers can still be acceptable even if the interference from some SUs is a bit higher, *i.e.* if some SUs select other bands different from ϕ_1. The potential benefit of giving more frequency band options to the SUs is to decrease the inter-SU interference, increasing the capacity of the secondary network.

Besides, when an SU tries to access the band of a close PBS, *i.e.* a band associated to a higher interference power such as ϕ_7, the SU can perform *PU activity detection* on the channels within the band [174]. This activity detection allows the SU to detect free channels before starting transmission, and to stop SU transmission when detecting overlap with PU transmissions as our mechanism in chapter 1 does. The closer the SU is to the PBS, the more reliable is the PU activity detection and therefore the less impact on PU communication. The free channels in ϕ_7 are identified as *temporal opportunities*.

The typical strategies of using only spatial opportunities (ϕ_1 channels) or only temporal ones (ϕ_7 free channels) are not optimal as we show in Fig. 2.2. The achievable capacity for SUs using these strategies is limited, because of inter-SU interference and the limitation in the number of available channels when using temporal opportunities.

Regarding PU degradation, note that the interference from the SUs using ϕ_7 or ϕ_6 may be very intense but, thanks to the PU activity detection in closer cells, it should be infrequent and last short periods of time (depending on the detection accuracy). On the other hand, the interference from the SUs using bands that usually do not allow PU activity detection (*e.g.,* ϕ_1 or ϕ_2) will be sustained over time, but will be less intense (similar to the co-channel interference from other PBSs). To properly adjust the vector $\boldsymbol{\rho}$ we should combine the effects of these two

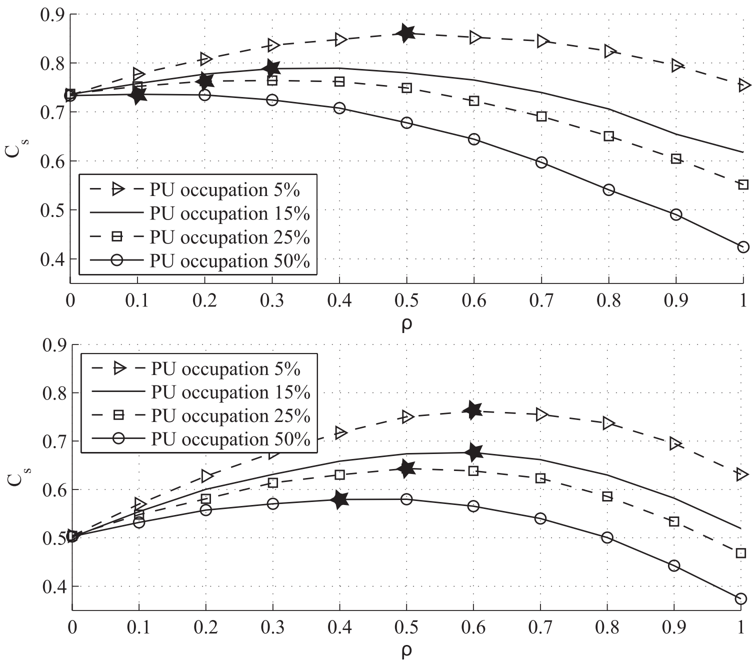

Figure 2.2: SU capacity versus ρ, the probability of using a temporal opportunity (and a spatial opportunity otherwise) under different PU traffic intensities. The number of new SU cognitive pairs at each time slot is generated by a binomial distribution characterized by 20 trials of 0.1 (top figure) and 0.2 (bottom figure) probability each. The rest of this reference scenario is described in section 2.5. The stars indicate the optimum SU capacity for each PU occupation.

types of interference into a single performance metric for the PUs: the probability of correct packet reception per time-slot.

Let R be the number of bands that an SU can use. We define the R-dimensional vector $\boldsymbol{\rho} = (\rho_1, \ldots, \rho_R)$, where ρ_i denotes the probability of using band ϕ_i, except for ρ_R which always corresponds to the probability of using band ϕ_7 (pure temporal access). Therefore, $0 \leq \rho_i \leq 1$ for $i = 1, \ldots, R$, and $\sum_{i=1}^{R} \rho_i = 1$. Let $\mathcal{P}$ denote the set of R-dimensional vectors fulfilling these conditions.

The following steps summarize the **system operation**:

1. The SAC periodically updates the vector $\boldsymbol{\rho}$ and sends it to the SUs.[1]

2. Each SU builds its own $\boldsymbol{\phi}$ vector by scanning the PBS pilot tones on each frequency band. This vector only needs to be updated when the SU changes its location.

3. Before transmitting, an SU randomly selects one band, ϕ_i from its $\boldsymbol{\phi}$ vector, according to the probability distribution $\boldsymbol{\rho}$, *i.e.* $P(\text{select band } \phi_i) = \rho_i$.

[1] It is advisable to divide the system into relatively homogeneous regions in terms of PBS density, traffic intensity and type of terrain, so that a suitable $\boldsymbol{\rho}$ can be found for each region.

4. If the SU is capable of detecting enough PBS power in ϕ_i to perform PU activity detection, then the SU tries to access over temporal opportunities, occupying only channels free of PU activity. Otherwise, the SU will access any channel with a sufficiently low SINR (considering also the interference from other SUs).

5. Periodically, the SAC retrieves information from both the primary and the secondary networks, particularly performance measures, which are taken into account to update vector $\boldsymbol{\rho}$.

This mechanism allows a semi-decentralized resource allocation. The SAC only needs to *announce* the vector $\boldsymbol{\rho}$ and retrieve small pieces of information measured at the terminals. The signaling overhead is therefore very low, especially compared to a centralized channel allocation by the SAC. If $\boldsymbol{\rho}$ is properly adjusted, the SUs will allocate themselves over the legacy spectrum, autonomously, efficiently, and with a low impact on the primary network. Moreover, $\boldsymbol{\rho}$ can be learned by the SAC with the RSM scheme explained in Section 2.4.

Next section formalizes the problem in terms of SU achieved capacity and PU probability of correct packet reception.

2.3 Problem Formulation

In this section we define the performance metrics for both the PUs and SUs and formulate the problem that the SAC needs to solve to determine the $\boldsymbol{\rho}$ vector.

Let us consider a secondary network with a given traffic intensity characterized by its arrival rate per area unit, and a random transmission time. As stated above, the vector $\boldsymbol{\rho}$ determines how the SUs distribute themselves over the available spectrum and the proportion of SUs using PU activity detection. In consequence, the SINR at each PU or SU receiver depends on $\boldsymbol{\rho}$. Let N_t^{SU} and N_t^{PU} denote the number of SUs and PUs in the system, respectively, at time-slot $t = 1, 2, \ldots$. The SINR over time at SU receiver $s \in \left\{1 \ldots N_t^{SU}\right\}$, is a discrete time stochastic process induced by $\boldsymbol{\rho}$, and denoted by $\Gamma_t^s(\boldsymbol{\rho})$. The expected normalized capacity per active SU pair is given by

$$C_s(\boldsymbol{\rho}) = E\left\{\lim_{T\to\infty}\frac{1}{T}\sum_{t=0}^{T}\sum_{s=1}^{N_t^{SU}}\frac{\log_2\left(1+\Gamma_t^s(\boldsymbol{\rho})\right)}{N_t^{SU}C_{\max}^S}\right\} \tag{2.1}$$

where $C_{\max}^S$ is the maximum achievable SU capacity per hertz. The expectation is taken over Γ_t^s and N_t^{SU}.[2] At a PU receiver, it is assumed that a data packet transmitted on time-slot t is correctly decoded if its SINR, Γ_t^{PU}, is greater than a given detection threshold, γ^{PU}. Then, the probability of correct detection at a PU

[2]Note that the traffic intensity in a cellular communication network varies during a day, but if it is observed during a smaller time window, *e.g.* 1 hour, the traffic arrival process can be considered stationary, with constant intensity.

is defined as

$$P_c(\boldsymbol{\rho}) = E\left\{\lim_{T\to\infty}\frac{1}{T}\sum_{t=0}^{T}\sum_{j=1}^{N_t^{PU}}\frac{\mathbb{I}_{\left\{\Gamma_t^j(\boldsymbol{\rho})>\gamma^{PU}\right\}}}{N_t^{PU}}\right\} \tag{2.2}$$

where Γ_t^j refers to the SINR process at the j-th active PU, and $\mathbb{I}_{\{z\}}$ is an indicator function which equals 1 if condition z holds, and equals 0 otherwise.

Therefore, the objective of the SAC is to find ρ solving the following problem:

$$\begin{aligned} \max_{\boldsymbol{\rho}} \quad & C_s(\boldsymbol{\rho}) \\ \text{s.t.} \quad & P_c(\boldsymbol{\rho}) \geq P_{c,\min} \\ & \rho \in \mathcal{P} \end{aligned} \tag{2.3}$$

where $P_{c,\min}$ denotes the minimum acceptable P_c.

Finding an optimal $\boldsymbol{\rho}$ is a challenging task because the (multiple) SINR stochastic processes capture the interaction of a random number of randomly located terminals with fading effects among each pair of them. Moreover, these processes and the decision vector $\boldsymbol{\rho}$, take values from continuous spaces, and therefore conventional dynamic programming techniques result infeasible. The problem (2.3) is, in fact, a *stochastic optimization problem with stochastic constraints* [183]. As usual in this type of problems, the SAC has to dynamically *learn* an optimal $\boldsymbol{\rho}$. One feasible way to address it is by means of Surface Response Methods (RSM) [184]. However, the inclusion of stochastic constraints introduces high complexity in the formulation. In the following section we develop the particular case in which $P_{c,\min}$ is sufficiently low for condition $P_c(\boldsymbol{\rho}) \geq P_{c,\min}$ to hold at the optimal $\boldsymbol{\rho}$ (in numerical results, $P_c(\rho)$ at the optimal ρ is never less than 5% of the P_c obtained in absence of SU access). This allows us to remove the stochastic constraint regarding $P_c(\boldsymbol{\rho})$. We leave as future work the inclusion of constraints in the RSM formulation.

2.4 Response Surface Method (RSM) Algorithm

The aim of the algorithm is the maximization of the expected value of the average capacity function (2.1) on a closed convex feasible domain $\mathcal{P} \subset \mathbb{R}^R$ for the input vector ρ, that is, to find a ρ approximately solving

$$\max_{\boldsymbol{\rho}\in\mathcal{P}} C_s(\boldsymbol{\rho}) \tag{2.4}$$

RSM allows us to find an approximate solution to this problem by successively estimating the gradient of the objective function and using these estimations in stochastic gradient ascent steps. At each one of these steps, numbered by $n = 1, 2, \ldots$, the system generates one update of the input vector $\boldsymbol{\rho}_{(n)}$ according to the following expression:

$$\boldsymbol{\rho}_{(n+1)} = \boldsymbol{\rho}_{(n)} + \alpha_{(n)}\hat{\nabla}C_s(\boldsymbol{\rho}_{(n)}) \tag{2.5}$$

where $\hat{\nabla}C_s$ denotes the estimation of the gradient ∇C_s, and $\alpha_{(n)}$ is the step-size weighting factor. A standard condition for the selection of $\alpha_{(n)}$, assuring the convergence of $\boldsymbol{\rho}_{(n)}$ [183], is $\sum_{n=1}^{\infty}\alpha_{(n)} = \infty$, $\sum_{n=1}^{\infty}\alpha_{(n)}^2 < \infty$.

Let us discuss the computation of $\hat{\nabla} C_s$. Given $\rho_{(n)}$ at step n, we consider a subdomain $\mathcal{S}_{(n)}$ of the feasible domain $\mathcal{P}$ such that $\boldsymbol{\rho}_{(n)} \in \mathcal{S}_{(n)} \subset \mathcal{P}$. Note that $\rho_{(n)}$ is the point at which the estimate $\hat{\nabla} C_s$ must be computed. Therefore, we need to estimate the objective function $C_s(\rho_{(n)})$ on $\mathcal{S}_{(n)}$, by taking samples $y^{(i)}$, $i = 1, \ldots, p$, of the function. For this, we need a finite set of points $\boldsymbol{\rho}_{(n,i)}$, $i = 1, \ldots, p$, generally called *design points*, belonging to $\mathcal{S}_{(n)}$. These points are chosen by the decision maker (the SAC in our case), and can be, for example, random perturbations of $\boldsymbol{\rho}_{(n)}$, falling within $\mathcal{S}_{(n)}$.

Let $t_{(n)}$ denote the time-slot in which the update $\rho_{(n)}$ is obtained. Given the set of p decision points, the SAC can obtain samples $y^{(i)}$ by this simple procedure:

1. Determine p sampling instants $t_{(n,i)} = t_{(n)} + iT$ for $i = 1 \ldots p$, where T is a sufficiently long time period for measuring performance at the SUs.

2. At $t_{(n,i-1)}$ (where $t_{(n,0)} = t_{(n)}$), the SAC signals the design point $\boldsymbol{\rho}_{(n,i)}$ to the SUs, for $i = 1 \ldots p$.

3. At $t_{(n,i)}$, the SAC obtains the capacity samples from each active SU and averages them to obtain $y^{(i)}$.

Thus, the estimates can be expressed as:

$$y^{(i)} = \frac{1}{T} \sum_{k=t_{(n,i-1)}}^{t_{(n,i)}} \sum_{s=1}^{N_k^{SU}} \frac{\log_2\left(1 + \Gamma_k^s(\boldsymbol{\rho}_{(n,i)})\right)}{N_k^{SU} C_{\max}^S} \qquad i = 1, 2, \ldots, p, \tag{2.6}$$

Note that the stochastic ascent algorithm needs p periods of length T to upgrade $\boldsymbol{\rho}_{(n+1)}$.

The objective function C_s is then approximated on $S_{(n)}$ by a polynomial response surface model $\hat{C}_s(\boldsymbol{\rho}) = \hat{C}_s(\boldsymbol{\rho}|\beta_0, \beta_1 \ldots \beta_R)$. The coefficients β_j, are determined by least squares estimation. Therefore, the RSM-gradient estimator $\hat{\nabla} C_s(\boldsymbol{\rho}_{(n)})$ at $\boldsymbol{\rho}_{(n)}$ is defined by the gradient (with respect to $\boldsymbol{\rho}$)

$$\hat{\nabla} C_s(\boldsymbol{\rho}_{(n)}) = \nabla \hat{C}_s(\boldsymbol{\rho}_{(n)}). \tag{2.7}$$

Thus, C_s is estimated on $S_{(n)}$ by the linear empirical model

$$\hat{C}_s(\boldsymbol{\rho}_{(n)}) = \beta_0 + \boldsymbol{\beta}_l^T(\boldsymbol{\rho} - \boldsymbol{\rho}_{(n)}) \tag{2.8}$$

where

$$\boldsymbol{\beta}^T = (\beta_0, \boldsymbol{\beta}_l^T) = (\beta_0, \beta_1, \ldots, \beta_R)^T \tag{2.9}$$

is the $(R+1)$-vector of unknown coefficients of the linear model. Having samples $y^{(i)}$ of the function values $C_s(\boldsymbol{\rho}_{(n,i)})$ at the design points $\boldsymbol{\rho}_{(n,i)}$, $i = 1, \ldots, p$, in $S_{(n)}$, we can obtain, by least squares, the following estimate $\hat{\boldsymbol{\beta}}$ of $\boldsymbol{\beta}$:

$$\hat{\beta} = (\mathbf{W}^T\mathbf{W})^{-1}\mathbf{W}^T\boldsymbol{y}. \tag{2.10}$$

Here, the $p \times (R+1)$-matrix $\mathbf{W}$ and the p-dimensional vector $\boldsymbol{y}$ are defined by

$$\mathbf{W} = \begin{pmatrix} 1 & \boldsymbol{\delta}^{(1)} \\ 1 & \boldsymbol{\delta}^{(2)} \\ \vdots & \vdots \\ 1 & \boldsymbol{\delta}^{(p)} \end{pmatrix}, \quad \boldsymbol{y} = \begin{pmatrix} y^{(1)} \\ y^{(2)} \\ \vdots \\ y^{(p)} \end{pmatrix} \tag{2.11}$$

with $\boldsymbol{\delta}^{(i)} = \boldsymbol{\rho}_{(n,i)} - \boldsymbol{\rho}_{(n)}$, for $i = 1, 2, \ldots, p$. Note that $(\mathbf{W}^T\mathbf{W})$ in (2.10) is invertible whenever the columns of $\mathbf{W}$ are linearly independent, which can be easily guaranteed by a proper selection of the design points.

In case $C_s(\boldsymbol{\rho})$ is concave on $\mathcal{P}$, the RSM algorithm will approach the global optimum following the stochastic gradient ascent iterations (2.5) as it has been observed for $R \geq 2$ dimensions in the scenarios considered in the following Section.

2.5 Numerical Results

Evaluation Framework

This subsection describes the Monte-Carlo methodology and the scenario used to evaluate C_s. The primary network uses a 7-band frequency planning, as previously stated, with irregular shaped cells having an average radius $r = 700$ m. We consider pathloss and multipath fading. To compute the pathloss attenuation over distance, $A(d)$ (dB), we use the following piecewise dual-slope model [125]:

$$A(d) = \begin{cases} K + 10\gamma_1 \log_{10}(d/d_0) & d_0 \leq d \leq d_c \\ K + 10\gamma_1 \log_{10}(d_c/d) + 10\gamma_2 \log_{10}(d/d_c) & d > d_c \end{cases} \tag{2.12}$$

The critical distance d_c is notably smaller for SU transmission than for PBS transmissions, because the PBSs are located at high outdoor locations while SUs are, in general, located either indoors or at ground level. All the signals are assumed to experience Rayleigh fading.

The area used to generate random terminal locations is a 4.2 km $\times$ 4.8 km rectangle. We focus on the downlink channels of one frequency band. We consider an scenario in which the primary traffic intensity is low 0.16 Erlangs/km^2, so that the average occupation of the spectrum by the primary terminals is only 5%. In contrast, the SU traffic intensity, 27.5 Erlangs/km^2, is high in comparison.

In this case, the SU capacity is mostly determined by the inter-SU interference and the RSM algorithm is essentially performing *interference management* in the SU network. We also discuss the effect of higher PU spectrum occupation and a different SU traffic intensity.

According to the ad-hoc nature of the secondary network, the average SU link distance considered is 90 m. Table 2.1 summarizes the simulation parameters considered.

Parameter	Assigned value
Primary transmitters	
number of downlink channels, N	5
cell radius, r	700 m
average received power at PU	-78 dBm
SINR detection threshold at PU,γ^{PU}	-17 dB
baseline noise at PU ($N_0 + I_{PU}$)	-110 dBm
Secondary transmitters	
average SU Tx power per channel	0.5 W
SU link distance	90 m
probability of PU activity detection	0.9
probability of overlap detection	0.8
Propagation parameters	
pathloss exponents, γ_1, γ_2	2.4, 4.2
propagation factor K	46.7 dB
critical distance for PBS transmission	$1.2r$ m
critical distance for SU transmission	100 m
RSM parameters	
dimensions of ρ,R	$1 \ldots 5$
measuring period T (in time-slots)	300
number of samples per step p	$3(2^{R-1}+1)$

Table 2.1: Parameter setting of the reference scenario used in numerical evaluations

Convergence and Usage of the Frequency Bands

Let us consider the case of 3-dimensional $\boldsymbol{\rho}$ vectors, $R = 3$. In this case, the ρ vector of a particular SU is $\rho = (\rho_1, \rho_2, \rho_3)$, being ρ_3 the probability of trying to access the band ϕ_7 of the primary cell where the SU is in, and ρ_1 and ρ_2 the probabilities of accessing ϕ_1 and ϕ_2, the bands where the SU receives less PBS power. The SU can only perform PU activity detection on ϕ_7 channels, while the channels of the other bands are considered spatial opportunities. Fig. 2.3 shows the values of ρ_1 and ρ_2 (ρ_3 is simply $1 - \rho_1 - \rho_2$) over consecutive update steps $n = 1, 2, \ldots$. The initial vector is $\boldsymbol{\rho}_{(0)} = (0, 0, 1)$. Although $\boldsymbol{\rho}_0$ is a rather poor initial guess, we see that the RSM algorithm stabilizes after 20 iterations. The final value is $\boldsymbol{\rho} = (0.29, 0.42, 0.29)$. Fig. 2.4 shows the estimated value of C_s as a function of ρ_1 and ρ_2. Consistently with the result obtained by RSM, the maximum values of C_s lie on the line $\rho_1 + \rho_2 = 0.7$.

Let us now consider the results for $R = 5$. The probability ρ_5 is now associated to ϕ_7, allowing PU activity detection, while $\rho_1 \ldots \rho_4$ are associated to $\phi_1 \ldots \phi_4$, where PU activity detection is assumed to be unfeasible. The initial $\boldsymbol{\rho}$ vector is $(0, 0, 0, 0, 1)$. Fig. 2.5 shows that, in this case, the convergence of RSM is as fast as with $R = 3$. Note that, as in the case of $R = 3$, the algorithm is not assigning ρ_1 the highest probability. The reason is that the algorithm aims to minimize inter

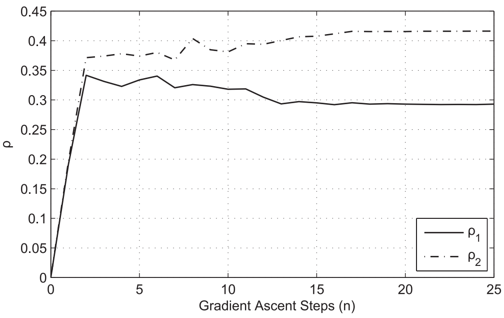

Figure 2.3: Consecutive RSM updates of ρ_1 and ρ_2.

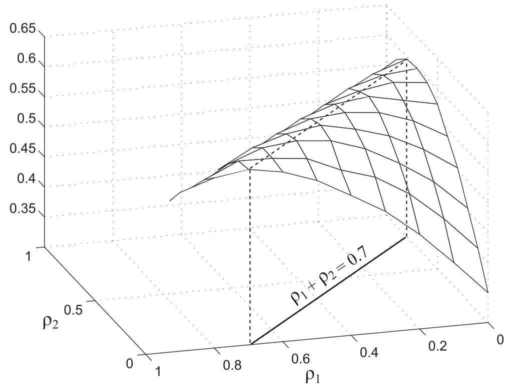

Figure 2.4: Estimation of C_s over ρ_1 and ρ_2.

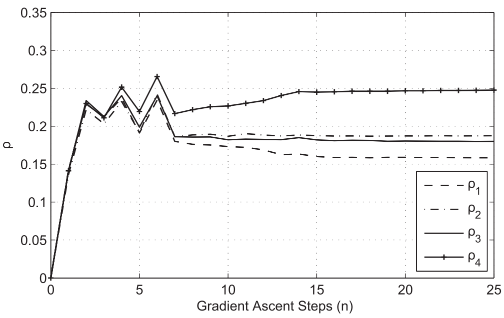

Figure 2.5: Consecutive RSM updates of $\rho_1 \dots \rho_4$.

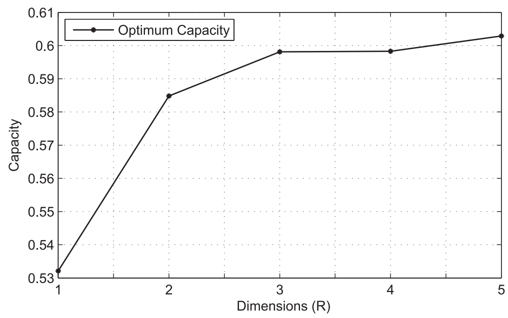

Figure 2.6: Maximum SU capacity obtained with RSM versus the number of dimensions of ρ, R.

SU interference by separating the SU transmitters using the same band. Recall that in Fig. 2.1 all the SUs in triangular region A shared the same ϕ_1 but had different values for ϕ_2. The aggregated probability of using spatial opportunities is $\sum_{i=1}^{4} \rho_i = 0.77$, which is higher than in the $R = 3$ case. This result confirms the idea that, the more spectrum is available to each SU, the more spectrum the SU exploits. Having more spectrum options per SU (higher R) also allows the SU network to achieve a higher capacity, as illustrated by Fig. 2.6.

Effect of the Traffic Intensity

Fig. 2.7 shows the average SU capacity attained by the RSM algorithm with $R = 2$, versus the average spectrum usage by the PUs, for different SU traffic intensities. As expected, the more spectrum occupied by PU traffic, the smaller the achieved capacity. Similarly, more SU traffic implies less SU capacity. The reason of the reduction on the maximum achieved capacity is the increment of the aggregate interference power at the SU receivers, from both the PBSs and other SU pairs. Compared to the typical approach of exploiting only temporal opportunities, the benefit of using RSM is noticeable for every traffic situation. In all cases, the reduction of the probability of correct detection at the PU receivers (P_c) was less than 5%.

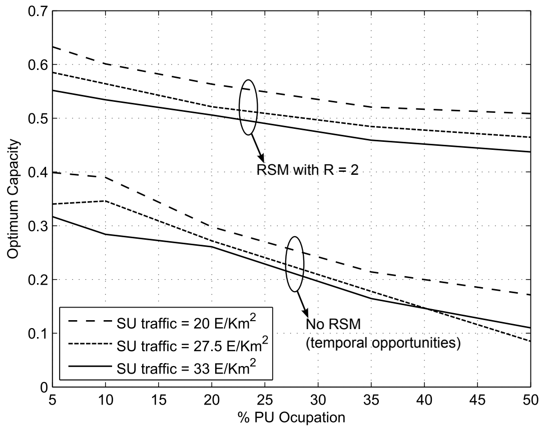

Figure 2.7: Maximum SU capacity obtained with RSM under different traffic intensities. For comparision, the figure also shows the capacity for a SU network exploiting only temporal opportunities (no RSM).

2.6 Conclusion

Motivated by the problem of spectrum reuse in cellular networks, we presented a semi-distributed mechanism allowing the secondary network to learn the most efficient spectrum access strategy. This mechanism exploits both spatial and temporal opportunities, and is especially effective for interference management in highly dense secondary networks. The learning approach is based on response surface methodology (RSM) which, according to our numerical results, improves notably the system capacity compared to usual strategies, and shows a fast convergence rate even when it is poorly initialized. Because of that, the system can adapt its control vector ρ to variations on the traffic intensity or user distribution. Surprisingly, to the best of our knowledge, the use of RSM on this framework had not been previously reported. Our future work is focused on incorporating performance constraints for the primary network in the RSM formulation.

Part II

Automated spectrum trading

Final conclusions

Bibliography

[1] FCC. (2002). Report of the spectrum efficiency working group. Techical report. FCC Spectrum Policy Task Force.

[2] Mitola, J., & Maguire, G. Q. (1999). Cognitive radio: making software radios more personal. *IEEE Personal Communications*, 6(4), 1318. doi:10.1109/98.788210

[3] Wang, B., & Liu, K. (2011). Advances in cognitive radio networks: A survey. *IEEE Selected Topics in Signal Processing*, 5(1), 523. doi:10.1109/JSTSP.2010.2093210

[4] Mayo, J. W., & Wallsten, S. (2010). Enabling efficient wireless communications: The role of secondary spectrum markets. *Information Economics and Policy*, 22(1), 6172. doi:10.1016/j.infoecopol.2009.12.005

[5] Yoon, H., Hwang, J., & Weiss, M. B. H. (2012). An analytic research on secondary-spectrum trading mechanisms based on technical and market changes. *Computer Networks*, 56(1), 319. doi:10.1016/j.comnet.2011.05.017

[6] Zhao, Y., Mao, S., Neel, J., & Reed, J. (2009). Performance evaluation of cognitive radios: Metrics, utility functions, and methodology. *Proceedings of the IEEE*, 97(4).

[7] Niyato, D., Hossain, E., & Han, Z. (2009). Dynamic spectrum access in IEEE 802.22-based cognitive wireless networks: a game theoretic model for competitive spectrum bidding and pricing. *IEEE Wireless Communications*, 16(2), 1623.

[8] Standard ECMA-392. (2009). MAC and PHY for Operation in TV White Space.

[9] Sun, C., & Tran, H.N., & Rahman, M. A., & Filin, S., & Alemseged, Y. D., & Villardi, G., & Harada, H. (2009). P802.19.1 Assumptions and Architecture

[10] IEEE 802.11 Working Group on Wireless Local Area Networks, `http://www.ieee802.org/11/` Accessed 10 July 2013

[11] IEEE P1900.5 Policy Language and Policy Architectures for Managing Cognitive Radio for Dynamic Spectrum Access Applications `https://ict-e3.eu/project/standardization/IEEE-SCC41.html` Accessed 10 July 2013

[12] Adler, J. (2012). Raging bulls: how Wall Street got addicted to light-speed trading. Wired.com. Retrieved from `http://www.wired.com/business/2012/08/ff_wallstreet_trading/all/` Accessed 15 June 2013

[13] Maharjan, S., Zhang, Y., & Gjessing, S. (2011). Economic approaches for cognitive radio networks: a survey. *Wireless Personal Communications*, 57(1), 3351. doi:10.1007/s11277-010-0005-9

[14] Hossain, E., Niyato, D., & Han, Z. (2009). *Dynamic spectrum access and management in cognitive radio networks*. Cambridge University Press.

[15] Niyato, D., & Hossain, E. (2008). Spectrum trading in cognitive radio networks: a market-equilibrium-based approach. *IEEE Wireless Communications*, (December), 7180.

[16] Niyato, D., & Hossain, E. (2008). Market-equilibrium, competitive, and cooperative pricing for spectrum sharing in cognitive radio networks: analysis and comparison. *IEEE Transactions on Wireless Communications*, 7(11), 42734283.

[17] Niyato, D., & Hossain, E. (2007). Hierarchical spectrum sharing in cognitive radio: a microeconomic approach. *IEEE Wireless Communications and Networking Conference, 2007.WCNC 2007.*, 38223826. doi:10.1109/WCNC.2007.699

[18] Niyato, D., & Hossain, E. (2007). Equilibrium and disequilibrium pricing for spectrum trading in cognitive radio: a control-theoretic approach. *IEEE Global Telecommunications Conference, 2007. GLOBECOM 07.*, 48524856. doi:10.1109/GLOCOM.2007.920

[19] Niyato, D., & Hossain, E. (2010). A microeconomic model for hierarchical bandwidth sharing in dynamic spectrum access networks. *IEEE Transactions on Computers*, 59(7), 865877.

[20] Xu, P., Kapoor, S., & Li, X. (2011). Market equilibria in spectrum trading with multi-regions and multi-channels. *IEEE Global Telecommunications Conference (GLOBECOM 2011)*, 2011, 04.

[21] Niyato, D., & Hossain, E. (2007). A game-theoretic approach to competitive spectrum sharing in cognitive radio networks. *IEEE Wireless Communications and Networking Conference*, 2007.WCNC 2007., 1620. doi:10.1109/WCNC.2007.9

[22] Mutlu, H., Alanyali, M., & Starobinski, D. (2008). Spot pricing of secondary spectrum usage in wireless cellular networks. *IEEE INFOCOM 2008. The 27th Conference on Computer Communications.*, 682690. doi:10.1109/INFOCOM.2008.118

[23] Wang, F., Krunz, M., & Cui, S. (2008). Price-based spectrum management in cognitive radio networks. *IEEE Journal of Selected Topics in Signal Processing*, 2(1), 7487. doi:10.1109/JSTSP.2007.914877

[24] Yu, H., Gao, L., Li, Z., Wang, X., & Hossain, E. (2010). Pricing for uplink power control in cognitive radio networks. *IEEE Transactions on Vehicular Technology*, 59(4), 17691778.

[25] Yang, L., Kim, H., Zhang, J., Chiang, M., & Tan, C. (2011). Pricing-based spectrum access control in cognitive radio networks with random access. *2011 Proceedings IEEE INFOCOM*, 22282236.

[26] Xu, D., Liu, X., & Han, Z. (2012). Decentralized bargain: a two-tier market for efficient and flexible dynamic spectrum access *IEEE Transactions on Mobile Computing*, 11. doi:10.1109/TMC.2012.130

[27] Huang, J., Berry, R. A., & Honig, M. L. (2006). Auction-based spectrum sharing. *Mobile Networks and Applications*, 11(3), 405418. doi:10.1007/s11036-006-5192-y

[28] Zhou, X., Gandhi, S., Suri, S., & Zheng, H. (2008). eBay in the Sky: strategy-proof wireless spectrum auctions. *Proceedings of the 14th ACM international conference on Mobile computing and networking . MobiCom 08*, 213.

[29] Huang, J., Han, Z., Chiang, M., & Poor, H. (2008). Auction-based resource allocation for cooperative communications. *IEEE Journal on Selected Areas in Communications*, 26(7), 12261237. doi:10.1109/JSAC.2008.080919

[30] Wang, X., Li, Z., Xu, P., Xu, Y., Gao, X., & Chen, H.-H. (2010). Spectrum sharing in cognitive radio networks–an auction-based approach. *IEEE transactions on systems, man, and cyberneticsPart B, Cybernetics*, 40(3), 58796. doi:10.1109/TSMCB.2009.2034630

[31] Gopinathan, A., Li, Z., & Wu, C. (2011). Strategyproof auctions for balancing social welfare and fairness in secondary spectrum markets. *2011 Proceedings IEEE INFOCOM*, 30203028. doi:10.1109/INFCOM.2011.5935145

[32] Zhu, Y., Li, B., & Li, Z. (2012). Truthful spectrum auction design for secondary networks. *2012 Proceedings IEEE INFOCOM*, 873881. doi:10.1109/INFCOM.2012.6195836

[33] Gandhi, S., Buragohain, C., Cao, L., Zheng, H., & Suri, S. (2008). Towards real-time dynamic spectrum auctions. *Computer Networks*, 52(4), 879897. doi:10.1016/j.comnet.2007.11.003

[34] Jayaweera, S. K., & Li, T. (2009). Dynamic spectrum leasing in cognitive radio networks via primary-secondary user power control games. *IEEE Transactions on Wireless Communications*, 8(6), 33003310. doi:10.1109/TWC.2009.081230

[35] Jayaweera, S. K., Vazquez-Vilar, G., & Mosquera, C. (2010). Dynamic spectrum leasing : a new paradigm for spectrum sharing in cognitive radio networks. *IEEE Transactions on Vehicular Technology*, 59(5), 23282339.

[36] Vazquez-Vilar, G., Mosquera, C., & Jayaweera, S. K. (2010). Primary user enters the game : performance of dynamic spectrum leasing in cognitive radio networks. *IEEE Transactions on Wireless Communications*, 9(12), 36253629.

[37] Duan, L., Gao, L., & Huang, J. (2011). Contract-based cooperative spectrum sharing. 2011 IEEE International Symposium on Dynamic Spectrum Access Networks, 399407.

[38] Ileri, O., Samardzija, D., & Mandayam, N. B. (2005). Demand responsive pricing and competitive spectrum allocation via a spectrum server. *2005 First IEEE International Symposium on New Frontiers in Dynamic Spectrum Access Networks, 2005. DySPAN 2005.*, 194202.

[39] Xing, Y., Chandramouli, R., & Cordeiro, C. (2007). Price dynamics in competitive agile spectrum access markets. *IEEE Journal on Selected Areas in Communications*, 25(3), 613621. doi:10.1109/JSAC.2007.070411

[40] Niyato, D., & Hossain, E. (2008). Competitive pricing for spectrum sharing in cognitive radio networks: dynamic game, inefficiency of Nash equilibrium, and collusion. *IEEE Journal on Selected Areas in Communications*, 26(1), 192202.

[41] Jia, J., & Zhang, Q. (2008). Competitions and dynamics of duopoly wireless service providers in dynamic spectrum market. *Proceedings of the 9th ACM international symposium on Mobile ad hoc networking and computing. MobiHoc 08*, 313322.

[42] Maille, P., & Tuffin, B. (2009). Price war with partial spectrum sharing for competitive wireless service providers. *IEEE Global Telecommunications Conference, 2009. GLOBECOM 2009.*, 1-6.

[43] Duan, L., Huang, J., & Shou, B. (2010). Cognitive mobile virtual network operator: investment and pricing with supply uncertainty. *2010 Proceedings IEEE INFOCOM*, (February 2009).

[44] Duan, L., Huang, J., & Shou, B. (2010). Competition with dynamic spectrum leasing. *IEEE Symposium New Frontiers in Dynamic Spectrum Access Networks 2010*, 111.

[45] Duan, L., & Huang, JianweiShou, B. (2011). Duopoly competition in dynamic spectrum leasing and pricing. *IEEE Transactions On Mobile Computing*, 11(11), 17061719.

[46] Duan, L., Huang, J., & Shou, B. (2011). Investment and pricing with spectrum uncertainty: a cognitive operators perspective. *IEEE Transactions on Mobile Computing*, 10(11), 15901604.

[47] Zhu, K., Niyato, D., Wang, P., & Han, Z. (2012). Dynamic spectrum leasing and service selection in spectrum secondary market of cognitive radio networks. *IEEE Transactions on Wireless Communications*, 11(3), 11361145. doi:10.1109/TWC.2012.010312.110732

[48] Guijarro, L., Pla, V., Tuffin, B., Maille, P., & Vidal, J. R. (2011). Competition and bargaining in wireless networks with spectrum leasing. *2011 IEEE Global Telecommunications Conference (GLOBECOM 2011)*, 16.

[49] Min, A., Zhang, X., Choi, J., & Shin, K. G. (2012). Exploiting spectrum heterogeneity in dynamic spectrum market. *IEEE Transactions on Mobile Computing*, 11(12), 20202032.

[50] Kim, H., Choi, J., & Shin, K. G. (2011). Wi-Fi 2.0: price and quality competitions of duopoly cognitive radio wireless service providers with time-varying spectrum availability. *2011 Proceedings IEEE INFOCOM*, 24532461. doi:10.1109/INFCOM.2011.5935067

[51] Tan, Y., Sengupta, S., & Subbalakshmi, K. P. (2010). Competitive spectrum trading in dynamic spectrum access markets: a price war. *2010 IEEE Global Telecommunications Conference. GLOBECOM 2010*, 15. doi:10.1109/GLOCOM.2010.5683358

[52] Dixit, S., Periyalwar, S., & Yanikomeroglu, H. (2010). A competitive and dynamic pricing model for secondary users in infrastructure based networks. *2010 IEEE 72nd Vehicular Technology Conference Fall (VTC 2010-Fall)*, 15. doi:10.1109/VETECF.2010.5594326

[53] Levent-Levi, T. (2012). Will MVNOs live long and prosper? Amdocs blogs. Retrieved from `http://blogs.amdocs.com/voices/2012/06/04/what-do-i-want-for-my-22nd-birthday-my-own-mvno-please/` Accessed 10 May 2013.

[54] Wang, S., Xu, P., Xu, X., Tang, S., Li, X., & Liu, X. (2010). TODA: Truthful Online Double Auction for spectrum allocation in wireless networks. *2010 IEEE Symposium on New Frontiers in Dynamic Spectrum (DySPAN)*, 110. doi:10.1109/DYSPAN.2010.5457905

[55] Niyato, D., Hossain, E., & Han, Z. (2009). Dynamics of multiple-seller and multiple-buyer spectrum trading in cognitive radio networks: a game-theoretic modeling approach. *IEEE Transactions on Mobile Computing*, 8(8), 10091022.

[56] Gao, L., Xu, Y., & Wang, X. (2011). MAP : Multiauctioneer Progressive auction for dynamic spectrum access. *IEEE Transactions on Mobile Computing*, 10(8), 11441161.

[57] Zhou, X., & Zheng, H. (2009). TRUST : a general framework for truthful double spectrum auctions. *IEEE INFOCOM 2009*, 9991007.

[58] Xu, H., Jin, J., & Li, B. (2010). A secondary market for spectrum. *2010 Proceedings IEEE INFOCOM*, 15. doi:10.1109/INFCOM.2010.5462277

[59] Jia, J., Zhang, Q., Zhang, Q., & Liu, M. (2009). Revenue generation for truthful spectrum auction in dynamic spectrum access. In *Proceedings of the*

tenth ACM international symposium on Mobile ad hoc networking and computing (pp. 312).

[60] Sengupta, S., Chatterjee, M., & Ganguly, S. (2007). An economic framework for spectrum allocation and service pricing with competitive wireless service providers. *2007 2nd IEEE International Symposium on New Frontiers in Dynamic Spectrum Access Networks*, 8998. doi:10.1109/DYSPAN.2007.19

[61] Sengupta, S., & Chatterjee, M. (2009). An economic framework for dynamic spectrum access and service pricing. *IEEE/ACM Transactions on Networking*, 17(4), 12001213.

[62] Kasbekar, G. S., & Sarkar, S. (2010). Spectrum auction framework for access allocation in cognitive radio networks. *IEEE/ACM Transactions on Networking*, 18(6), 18411854. doi:10.1109/TNET.2010.2051453

[63] Ji, Z., & Liu, K. J. R. (2008). Multi-stage pricing game for collusion-resistant dynamic spectrum allocation. *IEEE Journal on Selected Areas in Communications*, 26(1), 182191. doi:10.1109/JSAC.2008.080116

[64] Courcoubetis, C., & Weber, R. (2003). *Pricing communication networks: economics, technology and modelling*. Wiley.

[65] Yu, F. R. (2011). *Cognitive radio mobile ad hoc networks*. Springer.

[66] Liu, K., & Wang, B. (2010). *Cognitive radio networking and security: A game-theoretic view.* New York: Cambridge University Press.

[67] Hardin, G. (1968). The Tragedy of the Commons. *Science*, 162(3859), 12431248.

[68] Domenico, A. De, Strinati, E. C., & Di Benedetto, M.-G. (2012). A survey on MAC strategies for cognitive radio networks. *IEEE Communications Surveys Tutorials*, 14(1), 2144.

[69] Zhu, H., Pandana, C., & Liu, K. J. R. (2007). Distributive opportunistic spectrum access for cognitive radio using correlated equilibrium and no-regret learning. *IEEE Wireless Communications and Networking Conference, 2007.WCNC 2007.*, 1115.

[70] Maskery, M., Krishnamurthy, V., & Zhao, Q. (2009). Decentralized dynamic spectrum access for cognitive radios: cooperative design of a non-cooperative game. *IEEE Transactions on Communications*, 57(2), 459469.

[71] Myerson, R. B. (199). *Game theory: analysis of conflict*. Harvard University Press.

[72] Shen, S., Lin, X., & Lok, T. M. (2013). Dynamic Spectrum Leasing under uncertainty: A stochastic variational inequality approach. *2013 IEEE Wireless Communications and Networking Conference (WCNC)*, 727732. doi:10.1109/WCNC.2013.6554653

[73] Zhang, Y., Niyato, D., Wang, P., & Hossain, E. (2012). Auction-based resource allocation in cognitive radio systems. IEEE Communications Magazine, 50(11), 108120. doi:10.1109/MCOM.2012.6353690

[74] Yan, Y., Huang, J., & Wang, J. (2012). Dynamic bargaining for relay-based cooperative spectrum sharing. *IEEE Journal on Selected Areas in Communications*, (August), 14801493.

[75] Pan, M., Liang, S., Xiong, H., Chen, J., & Li, G. (2006). A novel bargaining based dynamic spectrum management scheme in reconfigurable systems. In *2006 International Conference on Systems and Networks Communications (ICSNC06)* (Vol. 00, pp. 5454). IEEE. doi:10.1109/ICSNC.2006.10

[76] Ji, Z., & Liu, K. J. R. (2006). WSN03-3: Dynamic pricing approach for spectrum allocation in wireless networks with selfish users. In *IEEE Globecom 2006* (pp. 15). IEEE. doi:10.1109/GLOCOM.2006.939

[77] Gao, L., Huang, J., & Shou B. (2013). An integrated contract and auction design for secondary spectrum trading. *IEEE Journal on Selected Areas in Communications*, (March), 581592.

[78] Vidal, J. R., Pla, V., Guijarro, L., & Martinez-Bauset, J. (2013). Dynamic spectrum sharing in cognitive radio networks using truthful mechanisms and virtual currency. *Ad Hoc Networks*, 11(6), 18581873. doi:10.1016/j.adhoc.2013.04.010

[79] Kim, S. (2013). A repeated Bayesian auction game for cognitive radio spectrum sharing scheme. *Computer Communications*, 36(8), 939946. doi:10.1016/j.comcom.2013.02.003

[80] Lee, K., Simeone, O., Chae, C.-B., & Kang, J. (2011). Spectrum leasing via cooperation for enhanced physical-layer secrecy. In *2011 IEEE International Conference on Communications (ICC)* (pp. 15). IEEE. doi:10.1109/icc.2011.5963501

[81] Elias, J., & Martignon, F. (2013). Joint operator pricing and network selection game in cognitive radio networks: equilibrium, system dynamics and price of anarchy. *IEEE Transactions on Vehicular Technology*, 62(9), 45764589.

[82] Galla, T., & Farmer, J. D. (2013). Complex dynamics in learning complicated games. *Proceedings of the National Academy of Sciences of the United States of America*, 110(4), 12326. doi:10.1073/pnas.1109672110

[83] Yan, Y., Huang, J., Zhong, X., Zhao, M., & Wang, J. (2011). Sequential bargaining in cooperative spectrum sharing: incomplete information with reputation effect. In *2011 IEEE Global Telecommunications Conference - GLOBECOM 2011* (pp. 15). IEEE. doi:10.1109/GLOCOM.2011.6134516

[84] F. Pantisano, *et. al.*, "Spectrum leasing as an incentive towards uplink macrocell and femtocell cooperation," *IEEE J. Select. Areas Commun.*, vol.30, no.3, pp.617-30, Apr. 2012.

[85] Yi, Y., Zhang, J., Zhang, Q., Jiang, T., & Zhang, J. (2010), "Cooperative communication-aware spectrum leasing in cognitive radio networks," *2010 IEEE Symposium on New Frontiers in Dynamic Spectrum*, Apr. 2010.

[86] Zhang, Z., Long, K., & Wang, J. (2013). Self-organization paradigms and optimization approaches for cognitive radio technologies: a survey. *IEEE Wireless Communications*, (April), 3642.

[87] Akkarajitsakul, K., Hossain, E., Niyato, D., & Kim, D. I. (2011). Game theoretic approaches for multiple access in wireless networks: a survey. *IEEE Communications Surveys & Tutorials*, 13(3), 372395. doi:10.1109/SURV.2011.122310.000119

[88] 1. Shoham, Y., Powers, R., & Grenager, T. (2007). If multi-agent learning is the answer, what is the question? *Artificial Intelligence*, 171(7), 365377. doi:10.1016/j.artint.2006.02.006

[89] T. M. Valletti, "Spectrum trading," *Telecommunications Policy*, vol. 25, no. 10-11, pp. 655–670, Oct. 2001.

[90] E. A. Jorswieck, L. Badia, T. Fahldieck, E. Karipidis, and J. Luo, "Spectrum sharing improves the network efficiency for cellular operators," *IEEE Commun. Mag.*, vol. 52, no. 3, pp. 129–136, Dec. 2013.

[91] Q. Zhao and B. Sadler, "A survey of dynamic spectrum access," *IEEE Signal Process. Mag.*, vol. 24, no. 3, pp. 79–89, May 2007.

[92] M. López-Martínez, J. J. Alcaraz, J. Vales-Alonso, and J. Garcia-Haro, "Automated spectrum trading mechanisms: Understanding the big picture," *Wireless Networks*, pp. 1–24, 2014, to be published.

[93] O. Simeone, I. Stanojev, S. Savazzi, U. Spagnolini, and R. Pickholtz, "Spectrum leasing to cooperating secondary ad hoc networks," *IEEE J. Sel. Areas Commun.*, vol. 26, no. 1, pp. 203–213, Jan. 2008.

[94] J. Zhang and Q. Zhang, "Stackelberg game for utility-based cooperative cognitive radio networks," in *Proceedings of the 10th ACM International Symposium on Mobile Ad Hoc Networking and Computing, (MobiHoc)*, 2009, pp. 23–31.

[95] G. Zhang, K. Yang, J. Song, and Y. Li, "Fair and efficient spectrum splitting for unlicensed secondary users in cooperative cognitive radio networks," *Wireless Personal Communications*, vol. 71, no. 1, pp. 299–316, Aug. 2012.

[96] M. López-Martínez, J. J. Alcaraz, L. Badia, and M. Zorzi, "Multi-armed bandits with dependent arms for cooperative spectrum sharing," in *IEEE International Conference on Communications ICC*, 2015, to be published.

[97] P. Auer, N. Cesa-Bianchi, and P. Fischer, "Finite-time analysis of the multi-armed bandit problem," *Machine learning*, vol. 47, no. 2-3, pp. 235–256, 2002.

[98] J. Gittins, K. Glazebrook, and R. Weber, *Multi-armed Bandit Allocation Indices*. West Sussex, UK: Wiley, 2011.

[99] X. Feng, G. Sun, X. Gan, F. Yang, and X. Tian, "Cooperative spectrum sharing in cognitive radio networks: A distributed matching approach," *IEEE Trans. Commun.*, vol. 62, no. 8, pp. 2651–2644, Aug. 2014.

[100] L. Duan, L. Gao, and J. Huang, "Cooperative spectrum sharing: A contract-based approach," *IEEE Trans. Mobile Comput.*, vol. 13, no. 1, pp. 174–187, Jan. 2014.

[101] Y. Yan, J. Huang, and J. Wang, "Dynamic bargaining for relay-based cooperative spectrum sharing," *IEEE J. Sel. Areas Commun.*, vol. 31, no. 8, pp. 1480–1493, Aug. 2013.

[102] Y. Yi, J. Zhang, Q. Zhang, T. Jiang, and J. Zhang, in *IEEE Symposium on New Frontiers in Dynamic Spectrum (DySPAN 2010)*, 2010, pp. 1–11.

[103] X. Yuan, Y. Shi, Y. T. Hou, W. Lou, and S. Kompella, "UPS: A united cooperative paradigm for primary and secondary networks," in *IEEE 10th International Conference on Mobile Ad-Hoc and Sensor Systems*, 2013, pp. 78–85.

[104] T. Nadkar, V. Thumar, G. Shenoy, A. Mehta, U. B. Desai, and S. N. Merchant, "A cross-layer framework for symbiotic relaying in cognitive radio networks," in *IEEE International Symposium on Dynamic Spectrum Access Networks (DySPAN)*, May 2011, pp. 498–509.

[105] Y. Han, S. H. Ting, and A. Pandharipande, *IEEE Trans. Wireless Commun.*, vol. 9, no. 9, pp. 2914–2923, Sep. 2010.

[106] D. Li, Y. Xu, X. Wang, and M. Guizani, "Coalitional game theoretic approach for secondary spectrum access in cooperative cognitive radio networks," *IEEE Trans. Wireless Commun.*, vol. 10, no. 3, pp. 844–856, Mar. 2011.

[107] D. Niyato and E. Hossain, "Market-equilibrium, competitive, and cooperative pricing for spectrum sharing in cognitive radio networks: Analysis and comparison," *IEEE Trans. Wireless Commun.*, vol. 7, no. 11, pp. 4273–4283, Nov. 2008.

[108] S. Jayaweera, M. Bkassiny, and K. A. Avery, "Asymmetric cooperative communications based spectrum leasing via auctions in cognitive radio networks," *IEEE Trans. Wireless Commun.*, vol. 10, no. 8, pp. 2716–2724, 2011.

[109] J. Alcaraz and M. van der Schaar, "Coalitional games with intervention: Application to spectrum leasing in cognitive radio," *IEEE Trans. Wireless Commun.*, vol. PP, no. 99, pp. 1–1, 2014.

[110] J. Huang, "Market mechanisms for cooperative spectrum trading with incomplete network information," *IEEE Commun. Mag.*, vol. 51, no. 10, pp. 201–207, Oct. 2013.

[111] A. Calvo-Armengol, "On bargaining partner selection when communication is restricted," *International Journal of Game Theory*, vol. 30, no. 4, pp. 503–515, Jan. 2002.

[112] T. T. Tran and H. Y. Kong, "Exploitation of diversity in cooperative spectrum sharing with the four-way relaying af transmission," *Wireless Personal Communications*, vol. 77, no. 4, pp. 2959–2980, Aug. 2014.

[113] D. B. Brown and J. E. Smith, "Optimal Sequential Exploration: Bandits, Clairvoyants, and Wildcats," *Operations Research*, vol. 61, no. 3, pp. 644–665, Jun. 2013.

[114] S. Pandey, D. Chakrabarti, and D. Agarwal, "Multi-armed bandit problems with dependent arms," in *ICML Proceedings of the 24th International Conference on Machine learning*, 2007, pp. 721–728.

[115] P. Si, H. Ji, F. R. Yu, and V. C. M. Leung, "Optimal cooperative internetwork spectrum sharing for cognitive radio systems with spectrum pooling," *IEEE Trans. Veh. Technol.*, vol. 59, no. 4, pp. 1760–1768, May 2010.

[116] M. Bkassiny, Y. Li, and S. K. Jayaweera, "A survey on machine-learning techniques in cognitive radios," *IEEE Commun. Surveys Tuts.*, vol. 15, no. 3, pp. 1136–1159, Oct. 2013.

[117] L. Gavrilovska, V. Atanasovski, I. Macaluso, and L. A. Dasilva, "Learning and reasoning in cognitive radio networks," *IEEE Commun. Surveys Tuts.*, vol. 15, no. 4, pp. 1761–1777, Mar. 2013.

[118] C. Shao, H. Roh, and W. Lee, "Aspiration level-based strategy dynamics on the coexistence of spectrum cooperation and leasing," *IEEE Communications Letters*, vol. 18, no. 1, pp. 70–73, Jan. 2014.

[119] A. Goldsmith, S. Jafar Ali, I. Maric, and S. Srinivasa, "Breaking spectrum gridlock with cognitive radios : An information theoretic perspective," *Proc. IEEE*, vol. 97, no. 5, pp. 894 – 914, May 2009.

[120] J. N. Laneman and G. W. Wornell, "An efficient protocol for realizing distributed spatial diversity in wireless ad-hoc networks," in *Proc. of ARL FedLab Symposium on Advanced Telecommunications and Information Distribution*, Washington, DC, 2001, pp. 294–.

[121] D. Bertsekas, *Dynamic Programming and Optimal Control*. Nashua, NH: Athena Scientific, 2000.

[122] P. Whittle, "Multi-armed bandits and the gittins index," *Journal of the Royal Statistical Society. Series B (Methodological)*, vol. 42, no. 2, pp. 143–149, 1980.

[123] S. Gass and T. Saaty, "The computational algorithm for the parametric objective function," *Naval Research Logistics*, vol. 2, no. 1-2, pp. 39–45, Mar. 1955.

[124] J. Vermorel and M. Mohri, "Multi-armed bandit algorithms and empirical evaluation," in *Machine Learning: ECML*, 2005, pp. 437–448.

[125] A. Goldsmith, *Wireless Communications*. Cambridge University Press, 2005.

[126] P. Pawelczak, *et. al.*, "Performance Analysis of Multichannel Medium Access Control Algorithms for Opportunistic Spectrum Access," *Vehicular Technology, IEEE Transactions on* , vol.58, no.6, pp.3014-3031, July 2009.

[127] A. De Domenico, E. Calvanese Strinati and M.G. Di Benedetto, "A Survey on MAC Strategies for Cognitive Radio Networks," *Communications Surveys & Tutorials, IEEE* , vol. 14, no. 1, pp. 21-44, 2012.

[128] J. Jia, Q. Zhang, X. Shen, "HC-MAC: A Hardware-Constrained Cognitive MAC for Efficient Spectrum Management," *Selected Areas in Communications, IEEE Journal on* , vol.26, no.1, pp.106-117, Jan. 2008.

[129] L. Gao, X. Wang, Y. Xu and Q. Zhang, "Spectrum trading in cognitive radio networks: a contract-theoretic modeling approach," *IEEE J. Selected Areas in Comm.*, 2011.

[130] J.P. Vasseur, M. Pickavet, and P. Demeester. "Network recovery: Protection and Restoration of Optical, SONET-SDH, IP, and MPLS." Morgan Kaufmann, 2004.

[131] R. Ramjee, R. Nagarajan, and D. Towsley. "On optimal call admission control in cellular networks," *IEEE INFOCOM*, 1996.

[132] J. Vazquez-Avila, F.A. Cruz-Perez and L. Ortigoza-Guerrero, "Performance analysis of fractional guard channel policies in mobile cellular networks," *IEEE Transactions on Wireless Communications*, vol. 5, no.2, Feb. 2006.

[133] Y.-C., Liang, K.-C. Chen, G.Y. Li, and P. Mhnen, "Cognitive radio networking and communications: An overview," *IEEE Trans. Veh. Technol.* vol. 60, no. 7, pp. 3386-3407, Sept. 2011.

[134] B. Wang, and K.J. Ray Liu, "Advances in cognitive radio networks: A survey," *IEEE Journal of Selected Topics in Signal Processing*, vol. 5n no. 1 pp. 5-23, Feb. 2011.

[135] X. Zhu, L. Shen, and T.-S.P. Yum., "Analysis of cognitive radio spectrum access with optimal channel reservation," *IEEE Comm. Letters*, vol. 11, no. 4, 304-306, Apr. 2011.

[136] J. Martinez-Bauset, V. Pla, D. Pacheco-Paramo, "Comments on "analysis of cognitive radio spectrum access with optimal channel reservation"," *IEEE Comm. Letters*, vol.13, no.10, pp.739, Oct. 2009.

[137] W. Ahmed, J. Gao, H. Suraweera, M. Faulkner, "Comments on "analysis of cognitive radio spectrum access with optimal channel reservation"," *IEEE Transactions on Wireless Communications*, vol.8, no.9, pp. 4488-4491, Sept. 2009.

[138] Lai, Jin, Ren Ping Liu, Eryk Dutkiewicz, and Rein Vesilo, "Optimal Channel Reservation in Cooperative Cognitive Radio Networks," in *IEEE 73rd Vehicular Technology Conference (VTC Spring)*, pp. 1-6, 2011.

[139] P.K. Tang, Y.H. Chew, L.C. Ong, M.K.Haldar, "Performance of secondary radios in spectrum sharing with prioritized primary access," in *Military Communications Conference, 2006*, IEEE MILCOM 2006, pp. 1-7. 2006.

[140] G. Wu, P.Ren, and Q. Du, "Recall-Based Dynamic Spectrum Auction with the Protection of Primary Users," *IEEE Journal on Selected Areas in Communications*, vol. 30, no. 10 pp. 2070-2081, 2012.

[141] E. Biglieri, et. al., "Principles of Cognitive Radio," Cambridge University Press, 2012.

[142] Chen Sun; G.P. Villardi, Zhou Lan, Y.D. Alemseged, H.N. Tran, H. Harada, "Optimizing the Coexistence Performance of Secondary-User Networks Under Primary-User Constraints for Dynamic Spectrum Access," *IEEE Trans. Veh. Technol.*, vol.61, no.8, pp.3665-3676, Oct. 2012.

[143] H. Kim. and K.G. Shin, "Efficient Discovery of Spectrum Opportunities with MAC-Layer Sensing in Cognitive Radio Networks," *Mobile Computing, IEEE Transactions on* , vol.7, no.5, pp.533-545, May 2008.

[144] W. Gabran, P. Pawelczak and D. Cabric, "Throughput and Collision Analysis of Multichannel Multistage Spectrum Sensing Algorithms," *Vehicular Technology, IEEE Transactions on* , vol.60, no.7, pp.3309-3323, Sept. 2011.

[145] H. T. Cheng, H. Shan and W. Zhuang; , "Stopping Rule-Driven Channel Access in Multi-Channel Cognitive Radio Networks," *2011 IEEE International Conference on Communications (ICC)*, pp.1-6, 5-9 June 2011.

[146] E. Jung and X. Liu, "Opportunistic Spectrum Access in Multiple-Primary-User Environments Under the Packet Collision Constraint," *Networking, IEEE/ACM Transactions on* , *in press* doi: 10.1109/TNET.2011.2164933.

[147] Q. Zhao, L. Tong, A. Swami and Y. Chen, "Decentralized cognitive MAC for opportunistic spectrum access in ad hoc networks: A POMDP framework," *Selected Areas in Communications, IEEE Journal on* , vol.25, no.3, pp.589-600, April 2007.

[148] S. Huang, X. Liu and Z. Ding, "Optimal Transmission Strategies for Dynamic Spectrum Access in Cognitive Radio Networks," *Mobile Computing, IEEE Transactions on* , vol.8, no.12, pp.1636-1648, Dec. 2009.

[149] S. Huang, X. Liu and Z. Ding, "Opportunistic Spectrum Access in Cognitive Radio Networks," *in Proc. IEEE INFOCOM 2008*, pp.1427-1435, 13-18 April 2008.

[150] J. Park, P. Pawelczak, and D. Cabric, "Performance of Joint Spectrum Sensing and MAC Algorithms for Multichannel Opportunistic Spectrum Access Ad Hoc Networks," *IEEE Transactions on Mobile Computing*, *in press* doi: 10.1109/TMC.2010.186

[151] Li, Yang, et al. "Optimal Myopic Sensing and Dynamic Spectrum Access in Cognitive Radio Networks with Low-Complexity Implementations," Wireless Communications, IEEE Transactions on 11.7 (2012): 2412-2423.

[152] W.S. Jeon, J.A. Han, and D. G. Jeong, "A novel MAC scheme for multichannel cognitive radio ad hoc networks," *IEEE Transactions on Mobile Computing*, vol. 11, no. 6, pp. 922-934, June 2012.

[153] D. Xu, E.J. Dan, and X. Liu, "Efficient and Fair Bandwidth Allocation in Multichannel Cognitive Radio Networks," *IEEE Transactions on Mobile Computing*, vol. 11, no.8, pp. 1372-1385, Aug. 2012.

[154] W. Rhee and J. M. Cioffi, "Increase in capacity of multiuser OFDM system using dynamic subchannel allocation," *in Proc. IEEE VTC*, vol. 2, pp. 1085-1089, May 2000.

[155] S. Sadr, A. Anpalagan and K. Raahemifar, "Radio Resource Allocation Algorithms for the Downlink of Multiuser OFDM Communication Systems," *IEEE Communications Surveys & Tutorials*, Vol. 11, No. 3, 2009.

[156] X. Gelabert, O. Sallent, J. Prez-Romero, and R. Agust, "Flexible Spectrum Access for Opportunistic Secondary Operation in Cognitive Radio Networks," *IEEE Transactions on Communications*, vol. 59, no. 10, pp. 2659-2664, Oct. 2011.

[157] L. Jiao, F.Y. Li, and V. Pla., "Modeling and Performance Analysis of Channel Assembling in Multichannel Cognitive Radio Networks With Spectrum Adaptation," *IEEE Transactions on Vehicular Technology*, vol. 61, no. 6, pp. 2686-2697, Jul. 2012.

[158] S. Tang and B. L. Mark, "Modelling and analysis of opportunistic spectrum sharing with unreliable spectrum sensing," *IEEE Trans. Wireless Commun.*, vol. 8, no. 4, pp. 1934-1943, Apr. 2009.

[159] D. Bertsekas, J. Tsitsiklis, "Introduction to Probability, 2nd Edition" Athenea Scientific, 2008.

[160] Solomon, H. "Geometric Probability," Philadelphia, PA: SIAM, 1978.

[161] P. Paweczak, *et. al*, "Quality of service assessment of opportunistic spectrum access: A medium access control approach," *IEEE Wireless Commun.*, vol. 15, no. 5, pp. 20-29, Oct. 2008.

[162] M. L. Puterman,*Markov Decision Processes: Discrete Stochastic Dynamic Programming*. Wiley-Interscience, Mar. 2005.

[163] D. Bolch, *et. al.*, 2006. *Queueing Networks and Markov Chains : Modeling and Performance Evaluation With Computer Science Applications* (2nd Edition). Wiley-Interscience.

[164] M. Masonta, M. Mzyece, N. Ntlatlapa, "Spectrum Decision in Cognitive Radio Networks: A Survey," *Communications Surveys & Tutorials, IEEE* , vol.PP, no.99, pp.1-20, 0 doi: 10.1109/SURV.2012.111412.00160.

[165] Q. C. Zhao, S. Geirhofer, L. Tong, and B. M. Sadler, "Opportunistic spectrum access via periodic channel sensing," *IEEE Trans. Signal Process.*, vol. 56, no. 2, pp. 785-796, Feb. 2008.

[166] Q. Zhao, L. Tong, A. Swami, and Y. Chen, "Decentralized cognitive MAC for opportunistic spectrum access in ad hoc networks: a POMDP framework," *IEEE J. Sel. Areas Commun.*, vol. 25, no. 3, pp. 589-600, Apr. 2007.

[167] Y. C. Liang, Y. H. Zeng, E. Peh, and A. T. Hoang, "Sensing-throughput tradeoff for cognitive radio networks," *IEEE Trans. Wireless Commun.*, vol. 7, no. 4, pp. 1326-1336, Apr. 2008.

[168] X. W. Zhou, J. Ma, G. Y. Li, Y. H. Kwon, and A. C. K. Soong, "Probability-based optimization of inter-sensing duration and power control in cognitive radio," *IEEE Trans. Wireless Commun.*, vol. 8, no. 10, pp. 4922-4927, Apr. 2009.

[169] W. Y. Lee and I. F. Akyildiz, "Optimal spectrum sensing framework for cognitive radio network," IEEE Trans. Wireless Commun., vol. 7, no. 10, pp. 3845-3857, Oct. 2008.

[170] J. Zhang, L. Qi, H. Zhu, "Optimization of MAC Frame Structure for Opportunistic Spectrum Access," *Wireless Communications, IEEE Transactions on* , vol.11, no.6, pp.2036-2045, June 2012.

[171] E. Jung, X. Liu, "Opportunistic Spectrum Access in Multiple-Primary-User Environments Under the Packet Collision Constraint," *Networking, IEEE/ACM Transactions on* , vol.20, no.2, pp.501-514, April 2012.

[172]

[173]

[174] E. Biglieri et.al., *Principles of Cognitive Radio*, Cambridge University Press, 2013.

[175] D. Tuan, B.L. Mark, "Joint spatial-temporal spectrum sensing for cognitive radio networks," , *IEEE Transactions on Vehicular Technology*, vol.59, no.7, pp.3480,3490, Sept. 2010

[176] Q. Wu et.al., "Spatial-Temporal Opportunity Detection for Spectrum-Heterogeneous Cognitive Radio Networks: Two-Dimensional Sensing," *IEEE Trans. on Wireless Commun.*, vol.12, no.2, pp.516-526, Feb. 2013.

[177] D. Guoru, et.al., "Joint exploration and exploitation of spatial-temporal spectrum hole for cognitive vehicle radios," *2011 IEEE International Conference on Signal Processing, Communications and Computing (ICSPCC)*, pp.1-4, Sep. 2011.

[178] M. G. Khoshkholgh, K. Navaie, and H. Yanikomeroglu, "Access strategies for spectrum sharing in fading environment: overlay, underlay and mixed," *IEEE Trans. Mobile Comput.*, vol. 9, no. 12, pp. 1780-1793, Dec. 2010.

[179] E. G. Larsson, M. Skoglund, "Cognitive radio in a frequency-planned environment: some basic limits," *IEEE Transactions on Wireless Communications*, vol.7, no.12, pp.4800-06, Dec. 2008.

[180] E. Axell, E.G. Larsson, D. Danev, "Capacity considerations for uncoordinated communication in geographical spectrum holes," *Physical Communication*, vol. 2, no.1, pp- 3-9, Mar. 2009.

[181] J. J. Alcaraz, J. A. Ayala-Romero, M. Lopez-Martinez, J. Vales-Alonso, "Combining Dual Tesselation and Temporal Access for Spectrum Reuse in Cellular Systems", *11th International Symposium on Wireless Communication Systems*, Aug. 2014.

[182] A. Goldsmith, *Wireless Communications*, Cambridge University Press, 2005.

[183] K. Marti, *Stochastic Optimization Methods*, Springer-Verlag, Berlin-Heidelberg, 2008.

[184] E. Angn et.al., *Response surface methodology with stochastic constraints for expensive simulation*, Journal of the Operational Research Society, 60 (6) (2009), pp. 735-746.